Aalto University
School of Engineering

Brian A. Nichols

Casting of Topologically Optimized Components Utilizing Additive Manufacturing

Master's thesis for the degree of Master of Science in Mechanical Engineering submitted for approval.

Espoo, May 29, 2017

Supervisor: Juhani Orkas, Professor, D.Sc.

Thesis advisor: Kalle Jalava, M.Sc.

Aalto University
School of Engineering

Aalto University, P.O. BOX 11000, 00076 AALTO
www.aalto.fi

Abstract of master's thesis

Author Brian A. Nichols

Title of thesis Casting of Topologically Optimized Components Utilizing Additive Manufacturing

Degree programme Mechanical Engineering

Major/minor Mechanical Engineering **Code** IA3027

Thesis supervisor Juhani Orkas

Thesis advisor(s) Kalle Jalava

Date 29.05.2017 **Number of pages** 65 **Language** English

Abstract: Casting is a widely-used metalworking method that is valued for its benefits in product manufacturability, repeatability, versatility, and low cost. Although casting capabilities are always improving, there are still many limitations in component design due to the constraints of conventional pattern fabrication methods. Topology optimization is an innovative design approach that optimizes the material layout of the designated geometry. Optimized designs are often too complex to manufacture with standard casting, machining, or other fabrication processes, forcing the utility of topology optimization to remain solely in preliminary design. These designs often require alteration to improve manufacturability, therefore diminishing the full potential benefits of the topology optimization. Additive manufacturing (AM) technologies, such as 3D printing, are capable of fabricating topologically optimized components without design alteration. However, the limited material selection offered by 3D printers inhibits the performance of printed components. Combining AM technologies and casting allows the possibility to manufacture topologically optimized components using typical casting alloys.

This work looks at current casting and AM technologies, the background of topology optimization, practical work on numerous original optimized designs, the adaption of selected designs to casting methodology, analysis of selected designs using casting simulations, and fabrication of selected designs via investment casting and sand mold casting. Results showed that the collaboration of casting and AM technologies allowed the fabrication of topologically optimized components without the need for significant design alteration. However, defects such as porosity and cracking occurred in both the simulations and physical castings of the components. These complications were likely caused by large variance in the size of adjacent features and by the presence of many flow fronts during pouring. Findings in this work highlight at least the following; optimized components can be produced by casting, although the methods and software need to develop further before the full potential of this approach can be reached. These issues could be mitigated through further study and optimization of the casting processes.

Keywords Casting, Topology Optimization, Additive Manufacturing, Rapid Prototyping, Investment Casting, Sand Mold Casting, 3D Printed Sand Mold, 3D Printing

Acknowledgements

I have much appreciation towards the country of Finland and to Aalto University for providing such an outstanding educational experience. The assistance and friendliness of the staff and students have been exemplary, setting a high bar for universities all over the globe. Special thanks goes to Juhani Orkas for being an excellent supervisor. His assistance and willingness to work with my tight schedule was highly commendable. The highest level of gratitude goes to Kalle Jalava for his superb work as my advisor. Even while juggling multiple roles at the university he managed to treat my work as highest priority. Kalle personally carried out the numerous castings needed for this work, which of course was very critical for my master's thesis. Attending the Mechanical Engineering Master's Degree Program the last two years and accomplishing this thesis work has been an amazing experience and I am extremely grateful for the opportunity. Thank you.

Espoo, May 29, 2017

Brian A. Nichols

Table of Contents

List of Figures

Nomenclature

ABS	*Acrylonitrile Butadiene Styrene*
AFS	*American Foundry Society (fineness number for aggregates)*
Al_2O_3	*Aluminum Oxide*
AlSi10	*Aluminum Silicon Alloy*
AM	*Additive Manufacturing*
CAD	*Computer-aided Design*
CAE	*Computer-aided Engineering*
CNC	*Computer Numerical Control*
DLP	*Digital Light Processing*
FDM	*Fused Deposition Modeling*
FE	*Finite Element*
FEA	*Finite Element Analysis*
IC	*Investment Casting*
Iso	*Isometric (view)*
PLA	*Polylactic Acid*
RP	*Rapid Prototyping*
SLA	*Stereolithography*
SLS	*Selective Laser Sintering*
UV	*Ultraviolet*
2D	*Two-Dimensional*
3D	*Three-Dimensional*

Tools Used

- SolidWorks 2015
- PTC Creo Parametric 3.0
- solidThinking Inspire 2017
- Magma5.3
- 3D Systems ProJet MJP 3600W wax printer
- Hetitec's voxeljet AG 3D sand printer

1 Introduction

Metal casting is among the oldest metalworking methods. Gradual technological advances have allowed the casting of newer metal alloys and more complex products. The increasing development of metal working methods and machining tools, especially with computer numerical control (CNC) and other automated tooling, further pushed the ability of casting methods by allowing the fabrication of complex patterns. The recent advances in 3D printing and rapid prototyping (RP) technologies has advanced metal casting capabilities even further. Cast products can now be manufactured utilizing 3D printed plastic patterns for mold fabrication. Recent development has allowed sand molds to be 3D printed directly, all but eliminating the need for pattern fabrication. The path from concept to cast product has never been faster than it is today. This is especially true with the advances in computer-aided design (CAD), finite element analysis (FEA), and other computer-based design and analysis methods.

Topology optimization is one of the more recent computer-aided engineering (CAE) methods that utilizes both design and structural analysis. Software optimizes model geometry in accordance to predetermined design constraints and applied loadings. This allows components to retain desired strength characteristics while minimizing volume. This approach also results in an improved strength/weight ratio of the component. The extremely complex geometry that can result from topology optimization causes difficult, and sometimes impossible, castability with traditional methods. One problem arises from design geometries that are impossible to machine using subtractive manufacturing methods. The other issue is the impossibility of pattern extraction from the mold.

Two methods to cope with these problems are investigated. Intricate wax or plastic patterns can be 3D printed for use in investment casting. The lower melting point of these materials (ABS, PLA, wax) relative to the ceramic mold allows the plastic to be melted and drained, easing the removal of complex patterns. A different approach is applied to sand mold casting. Complex sand molds and/or cores are 3D printed, which eliminates the need for a pattern.

Utilizing such complex molds may cause other complications. Intricate geometry can cause problems such as premature cooling in small channels, flow front collisions, riser and sprue placement difficulty, and complicated parting lines. This work investigates such variables in order to evaluate the castability of aluminum when using complex topologically optimized molds.

1.1 Purpose

Casting is a versatile fabrication method with many of the benefits relating to manufacturability, repeatability, and optimal production speed. Complicated designs can cause difficult pattern machinability. Current methods typically require design alterations in order to make pattern production and casting possible. This often diminishes optimized component geometry. Topologically optimized designs are similarly simplified in order to be manufacturable. This causes topology optimization to be useful only as preliminary design. However, improved casting capability provided by RP technologies and the ability

to directly 3D print sand molds might allow topologically optimized products to be cast without alteration. This study explores the capability of casting complex topologically optimized designs.

1.2 Approach

This work consists of multiple sections addressing different aspects of the thesis. The completion of these sections was largely chronological. The order of completion of both the work and paper relied heavily on knowledge acquisition, apparatus availability, and product development path. The composition of this paper and the experimental work were accomplished concurrently in order to achieve optimal documentation and time management. The project tasks are shown below.

1. Topic assignment and definition
2. Background information research and resource acquisition
3. Start of paper composition
4. Preliminary product design and optimization
5. Design selection and post-optimization development
6. Flow, temperature, and solidification simulations
7. Casting of chosen designs
8. Presentation of finished work

1.3 Delimitation

The scope of this work encompasses many disciplines. However, the discussion of these disciplines is minimal or exempt due to content irrelevance or timeline confliction. These subjects are shown below.

- Applied forces – loading, supporting, and other similar parameters are required in order to topologically optimize a design. The presentation of these values are optional; these details are of little importance. In general, these values were assigned in a logical manner according to the component's size, material, function, etc.
- Structural analysis – FEA or other structural analysis methods are not conducted on product designs nor on finished products. The primary focus of this work is on the relationship between design complexity and castability. The physical performance of the finished components is not in the scope of this work.
- Casting optimization – Casting of the components is accomplished but the process is not optimized in this work. Casting simulations are also completed but not optimized. The processes in this work are proof of concept.
- Casting of some designs – Two designs were chosen for casting; one for investment casting (propeller hub) and one for 3D printed sand mold casting (lower A-arm). Timeline constraints did not allow casting of the 3D printed sand mold component (lower A-arm). However, the component design and mold design were both finalized and presented in this work.

2 Background

2.1 Topology Optimization

Structural mechanics is a vital discipline in the engineering field. Although methodology has remained largely unchanged for decades, the constant demand for stronger and lighter products has resulted in the emergence of new analytical approaches and techniques. Topology optimization is a relatively new method in this field. Basic principles were defined in the early twentieth century in the form of truss analysis. Topology optimization advanced with the development of optimal layout theory in the late 1970's. This technique continued to improve with FE-based shape optimization in the 1990's. The exponential increase in computer computational speed has greatly improved the capability of topology optimization methods. [1]

The general purpose of topology optimization is to reduce the mass of an object while maintaining optimal strength and stiffness characteristics. Predefined parameters determine the level of optimization. Many of these parameters are similar to those required for finite element analysis: support properties and locations, applied loading, material properties, desired mass percentage, and design space.

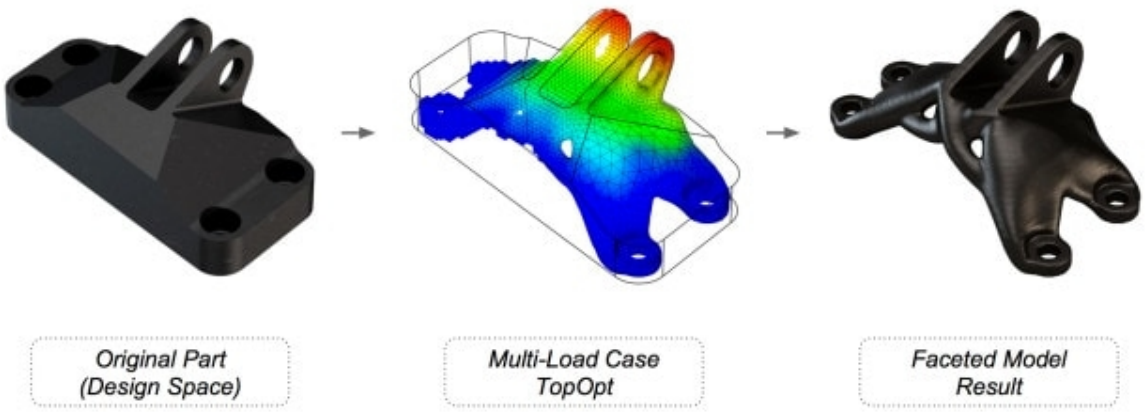

Figure 1: Topology optimization example with simple bracket [2]

Topology optimization exists in the domain of 3D modeling. Prior to optimization, the component design is either created in an alternate CAD program and imported into the topology optimization software or may be created in the topology optimization software directly. Additional parameters are then defined in order to proceed with the optimization. The analysis often results in a rough surface finish that can be smoothed with other tools that are included in the program.

The fabrication of topologically optimized components has only been plausible in recent years. The resulting design is often too complex to manufacture using machining techniques, either manual or automated. These complex designs are also very difficult to fabricate using common casting methods. Only the emergence of 3D printing and other AM techniques has

allowed the direct fabrication of topologically optimized components. Recent collaboration between 3D modeling and topology optimization programs aims to exploit the full potential of AM technologies [2]. Other opportunities such as design competitions (Figure 2) push AM innovation even further as modeling and optimization programs become more refined and accessible.

Figure 2: The Generate Quadcopter Challenge promotional photo [3]

The physical properties of these printed materials (plastics and waxes) are limited due to relatively poor strength, durability, and thermal characteristics. Metal SLS printed components solve some of these problems but come with high expense and long production time. Direct casting of topologically optimized components has the potential to solve all of these problems.

2.2 Casting

The metal casting process has deep roots in the history of product manufacturing. The emergence of smelting copper for lost wax casting was the beginning of the growth of all other casting methods. The first instances of copper castings originated around 4000 B.C as separate instances in locations such as Anatolia, Iran, Syria, Palestine, and Thailand. This new technology was the start of the Bronze Age. [4]

Many other casting methods have been developed over time, each having their own strengths and weaknesses as manufacturing processes. Some of the most utilized methods are die mold casting, continuous casting, permanent mold casting, sand casting, and investment casting. The latter two methods were utilized in this work.

2.2.1 Investment Casting

Investment casting (IC) is defined by pouring molten metal into a ceramic shell mold. The surface quality of investment cast components is quite high due to the construction process and material composition of the mold. Ceramic molds are inert; meaning the interaction between mold and cast material is non-existent or very low.

The IC process begins with the fabrication of a consumable wax pattern. The common method is to inject wax into a reusable tool. This tool is often machined from metal and must have at least one parting line in order to remove the formed wax pattern. Factors such as these limit tool and pattern geometries.

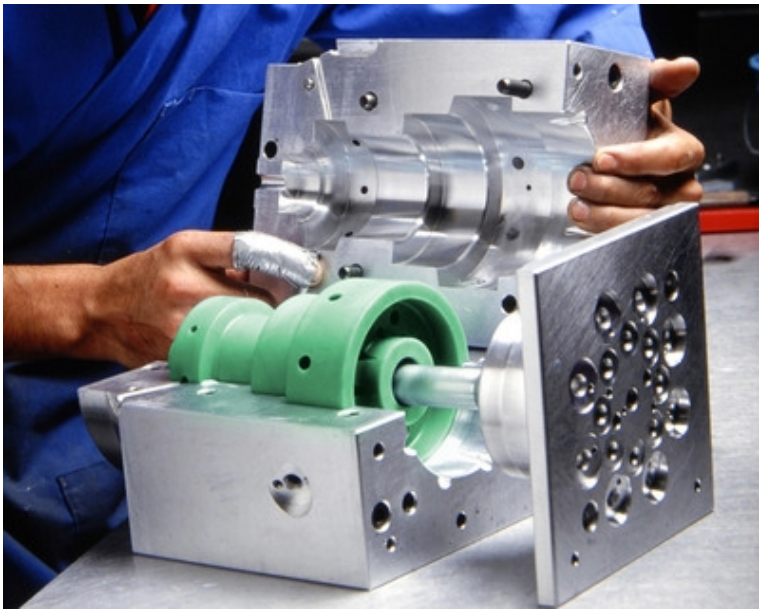

Figure 3: Example of wax pattern and tool [5]

The mold begins as a liquid slurry consisting of a finely powdered mineral and a binder. The powdered mineral is often aluminum silicate or zircon. This slurry coats a wax pattern in multiple layers. Each slurry layer is applied, coated with a coarser material (sand and/or stucco), and then dried. Once the mold has the desired number of layers, the wax is burned out and the mold shell is fired at a high temperature (usually 1000°C or higher) for a final curing and hardening[1] [6]. Pre-heating of the ceramic mold can be performed to facilitate filling. This is especially helpful when small channels or features are present. The mold is removed after the metal has solidified and cooled sufficiently. This is usually accomplished with the destruction of the mold since it is a single piece with no parting lines.

[1] This process is credited for the *lost wax* term that is often associated with investment casting. [6]

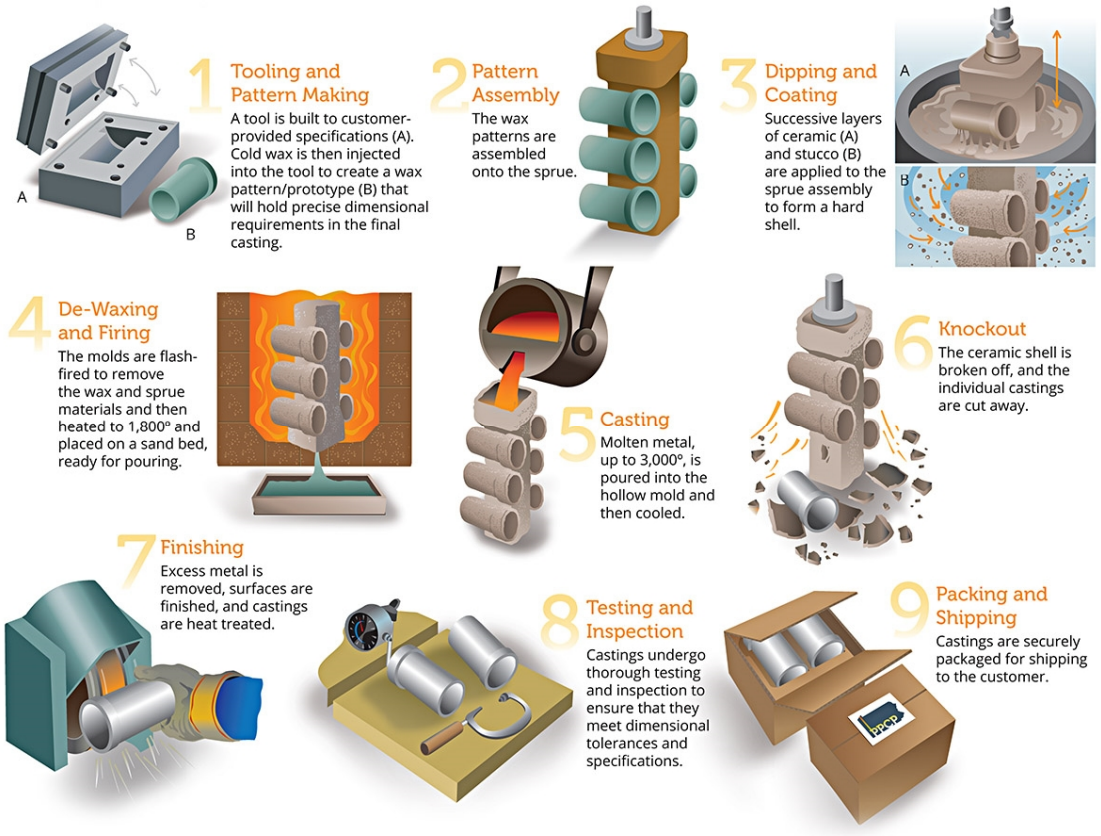

Figure 4: Investment casting process [7]

The investment casting process does present a few negative characteristics. For example, removal of the ceramic shell can be a risky process, especially when the component material is soft or fragile. Ceramic molds are also prone to cracking that can lead to product defects and sometimes complete destruction of the mold. This cracking can occur at any point in the investment casting process: wax burnout, firing, pouring, and cooling. Investment casting molds cannot be reused, which drives up manufacturing time and cost. [6]

2.2.2 Sand Mold Casting

Sand mold casting is a fast, cheap, and widely used casting process. Sand molds are made from various aggregate/binder combinations. Greensand (as opposed to dry sand) molds consist of an aggregate that is bonded with a clay (bentonite) and water mixture. This form of sand mold is environmentally friendly and can be recycled and reused relatively easily. It is also very cheap and can manufacture products very quickly. Modern plants can produce up to 600 greensand molds per hour. This is significantly faster than the production of chemically bonded molds, which top out at around 100 molds per hour. [6]

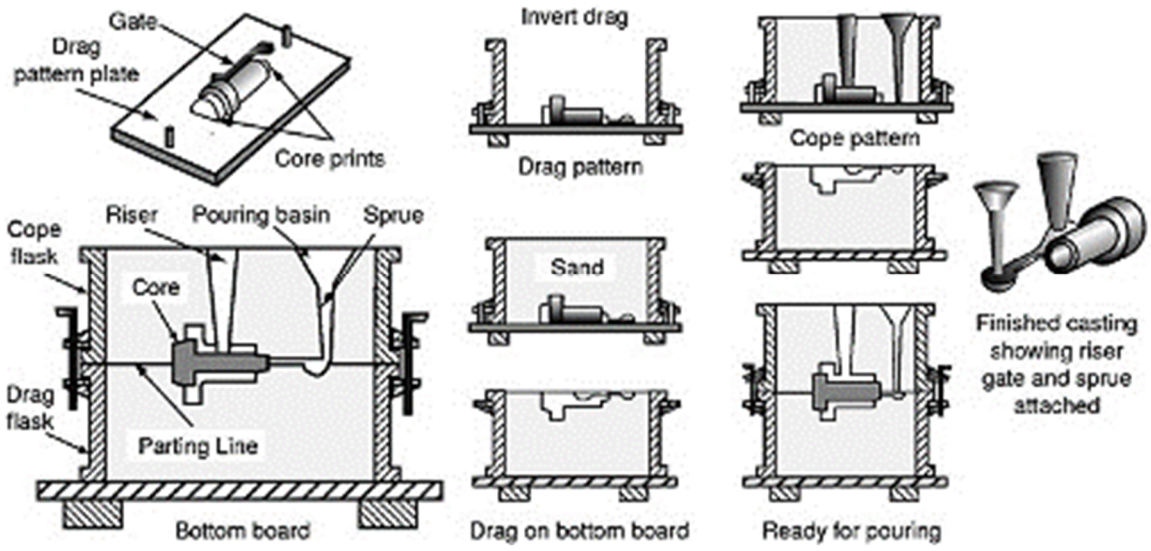

Figure 5: Sand mold casting process [8]

Many different aggregates can be used in sand molds. Silica sand, chromite sand, olivine sand, and zircon sand are a few of the more commonly used aggregates[2]. These materials present differences in characteristics such as mold expansion, mold/metal reactions, and mold consumption and reusability. Aggregates can also be found in different grain sizes. The unit for average grain size is denoted as AFS (American Foundry Society) fineness number for aggregates [9]. Since this unit is somewhat arbitrary, the following equation is used to establish the average diameter of the grains.

$$AFS\ number \times micrometers = 15{,}000$$

A higher AFS number results in smaller average grain size. For example, AFS 100 has an average grain size of 150 μm while AFS 200 has an average grain size of 75 μm. Surface finish characteristics are heavily dependent on the AFS fineness number. [6]

The main disadvantage of greensand casting is the 'greenness' of the molds. The molds are relatively plastic in nature, which makes them prone to distortion. This can be avoided with proper mold consolidation. Another side effect is the absorption of water from the mold into its cores. This can be avoided by limiting the time between mold assembly and pouring. [6]

[2] Many of the aggregates used in sand molds are not actually sand. Aggregate molds would be a more accurate title. Although this may be true, most aggregates are referred to as sand. [6]

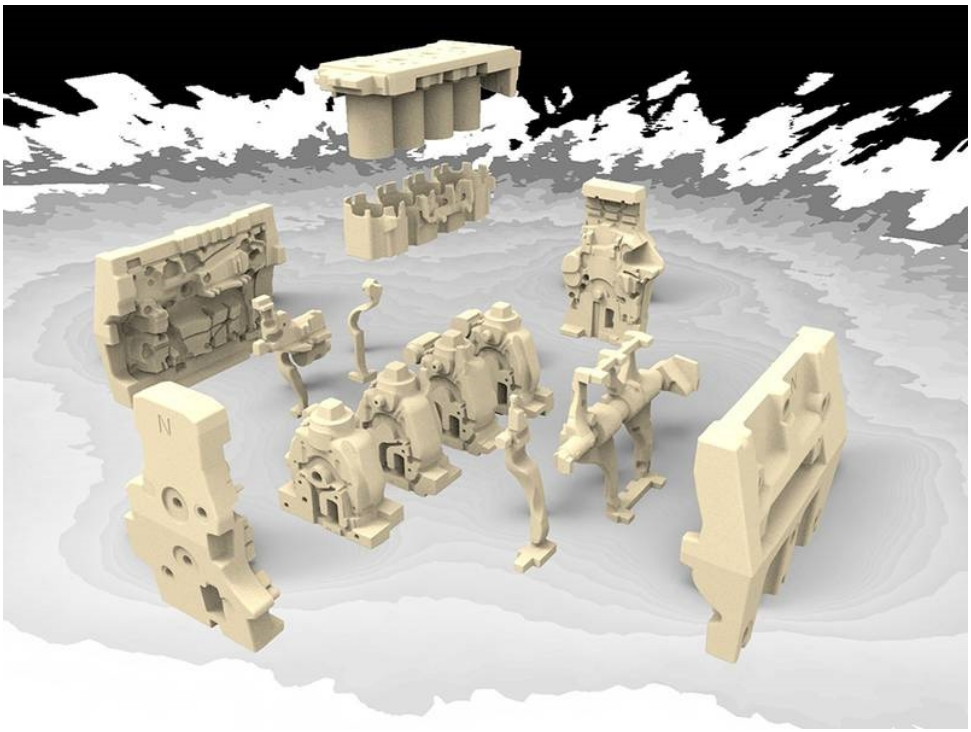

Figure 6: Cores for a sand mold engine casting [10]

The capabilities of sand mold casting is commendable. Components of various shapes, sizes, and complexities can be fabricated using sand mold casting. The inclusion of sand cores and the ability to create multiple-piece molds allow the manufacturing of highly complex components.

2.3 Rapid Prototyping and Additive Manufacturing

Rapid prototyping technologies have become an integral part of product development in many industries. The term encompasses the design, analysis, and prototyping stages of product development. The fabrication of prototypes is often required in order to optimize products in areas that computer modeling and simulation cannot. Because the modeling, analysis, and prototyping process is iterative, the time consumed during these stages is crucial. The emergence and constant improvement of CAD programs, analysis and simulation software, and AM technologies have greatly reduced the time required for these stages. Rapid prototyping therefore allows the smallest amount of time between product conception to product completion. [11]

2.3.1 Stereolithography

Stereolithography (SLA) was the first commercially available 3D printing technology [12]. This additive manufacturing method uses focused ultraviolet (UV) laser to solidify a liquid or powder medium. Acrylates and epoxies are some of the more commonly used photopolymerizable polymers [13]. Ultraviolet light solidifies and bonds the medium in sequential 2D layers until the component is fully formed. These layers are solidified either by laser scanning or with mask image projection. The latter uses a digital light processing (DLP) projector to solidify each layer entirely, which facilitates faster print times [14].

Components printed using SLA often have higher resolution and smoother surface finish than components printed by FDM machinery. While stereolithography has its advantages in the realm of rapid prototyping, its utilization with investment casting is not ideal. This is mainly due to the high melting[3] temperature and high thermal expansion coefficient of the resins used. This expansion rate is higher than the plastics used with FDM and much higher than the IC ceramic molds. This leads to case cracking during the burnout stage. Studies addressing this problem have shown that the implementation of special lattices within the SLA printed patterns can alleviate these stresses on the casing. [15] [16]

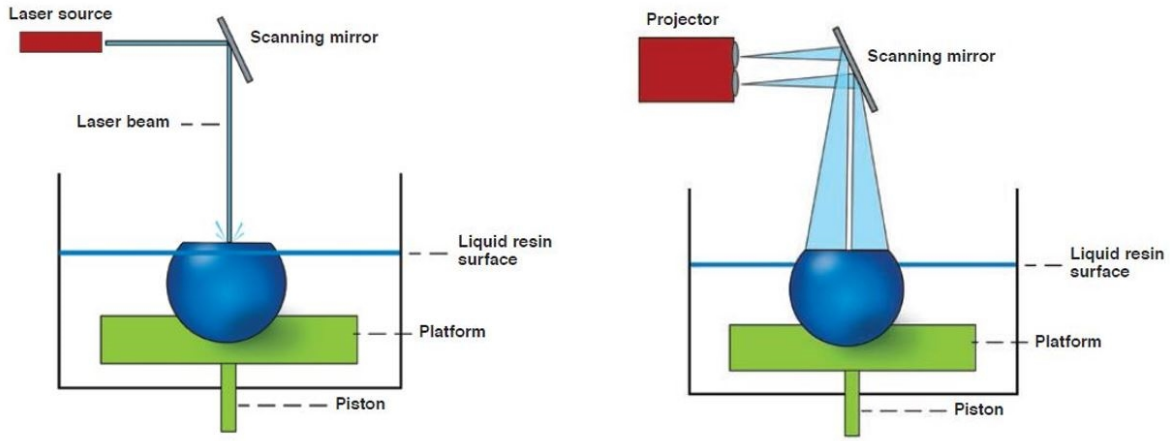

Figure 7: Laser scanning and DLP stereolithography 3D printers [17]

2.3.2 Selective Laser Sintering

Selective laser sintering (SLS) is a variation of laser scanning stereolithography 3D printing; similarly, it uses a high-powered laser to solidify and bond the medium material. The mediums associated with SLS, however, are almost exclusively metal alloys in powder form. This material niche also places SLS printing in an alternative market than most other AM technologies. The RP benefits exhibited by SLS are similar to FDM and stereolithography. They differ due to SLS components' higher potential for direct implementation. This potential is largely due to the material, which typically offers higher strength characteristics than polymers. Selective laser sintering has not established itself as a high-volume manufacturing method due to high production cost, long lead-time, and the relatively minimal material selection compared to casting and other manufacturing methods. For these reasons, SLS printing is not an ideal method for mass manufacturing of topologically optimized components. Objects printed with SLS do not make good patterns for investment casting either because the high melting point causes extreme difficulties during the burnout process. Although topologically optimized components can be created using SLS with relative ease, high cost and long lead-times cause overall manufacturability to be poor. [18]

[3] The resin does not actually melt, but burns out. This occurs around 1200°C with proper oxygen exposure. [16]

2.3.3 Fused Deposition Modeling

Fused deposition modeling (FDM) is a relatively new form of additive manufacturing. This method feeds plastic filament through a heated nozzle that melts and distributes it layer by layer. With most FDM printers, this nozzle (Figure 8) moves in the X and Y directions while the build platform manipulates the Z direction. Sequential 2D layers are stacked and bonded until the product is finished.

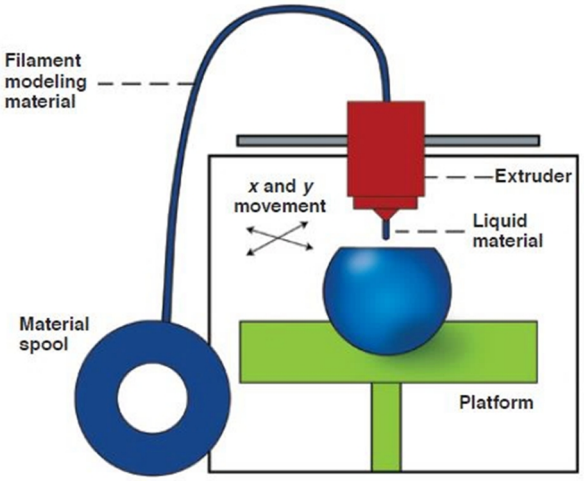

Figure 8: Basic FDM 3D printer [17]

The accuracy of current machinery is commendable (easily in the sub-0.1 mm range) and continually improving [19]. The level of accuracy depends heavily on the quality and cost of the machine, which can range from around one thousand dollars up to one hundred thousand dollars [17]. This vast range represents 3D printers of many sizes, qualities, and purposes, allowing them to have a place in both consumer and industrial markets. The FDM printer material selection is also quite large. Many plastics and waxes are available, often in many different colors and finishes. Some of the more recently developed materials are hybrids. For example, a Nylon-6 polymer reinforced with Al_2O_3 for strength and casting benefits [20].

2.4 Casting and AM Technologies

The developing collaboration of casting and AM technologies over the past decade has proven to be very beneficial in applicable scenarios. Rapid prototyping of cast components is one such scenario. The RP abilities offered by 3D printed plastics and waxes have been applied to multiple casting methods. The benefits are arguably the greatest with investment casting where AM technologies can assist directly or indirectly. The indirect approach utilizes additive manufacturing methods to fabricate the pattern mold. This mold is then used to create the consumable wax patterns for investment casting. The direct approach eliminates the need for a pattern mold by 3D printing the consumable wax pattern. [21] [22]

The low melting temperature and low thermal expansion of ABS, PLA, and wax make the burnout process quick and easy. The low thermal expansion helps reduce the chance of mold

cracking when paired with proper application of slurry and aggregate [23]. Unlike SLA patterns, patterns made with ABS, PLA, and wax also do not require an internal lattice structure to cope with thermal expansion [15]. The finished components show results (dimensional accuracy, surface finish, porosity, etc.) comparable to components made using traditionally fabricated patterns. [24] [25]

Thermal properties	PLA	ABS
Melt volume index (MVI)	10.3 cm³/10min	9.7cm³/10min
Glass transition temperature	60-65°C	105°C
Slumping temperature	70-80°C	110-125°C
Melting temperature	160-190°C	210-240°C
Printing temperature	190-220°C	230-250°C
Recommended printbed temperature	50-70°C (heated bed not mandatory)	80-120°C (heated bed required)

Figure 9: Thermal properties of PLA and ABS [26]

The collaboration of sand mold casting and AM technologies has also proven beneficial. Because the sand mold casting process does not necessitate the burnout stage required during investment casting, the only benefit that AM lends to sand mold manufacturing is fast and easy pattern fabrication. Pattern fabrication is accomplished with 3D printing rather than with traditional methods such as CNC machining or other more time-intensive fabrication methods. [27]

Overall, AM technologies improve the prototyping abilities of casting methods. The time required for the entire casting process is reduced due to the relatively small amount of time required to fabricate a printed pattern. This benefit is further realized during product development when numerous design iterations need to be cast. Although the current benefit towards mass manufacturing is relatively small, AM technologies can greatly improve the casting process optimization of new components. The use of AM technologies also benefits low volume production of specialized cast products by increasing production speed, allowing more complex castings, and reducing production costs. [28] [29]

The collaboration of AM technologies and casting has made casting practices more accessible to non-commercial parties. The emergence of affordable 3D printers has allowed easy access to the design and fabrication of plastic components that previously required injection molding or other commercial fabrication processes [30]. The applications of 3D printing have developed from solely prototyping to direct component fabrication. The technology has recently found a place in casting processes as a quick, easy, and cheap pattern fabrication method. All of these developments have made casting technologies much more accessible and appealing to home projects, new businesses, and established industries. [31] [32]

The collaboration of casting and AM technologies has also allowed the possibility of more geometrically complex casting. The ability of AM technologies to fabricate extremely complex geometries that are otherwise difficult or impossible to produce using subtractive manufacturing methods has shown promise to carry over to casting practices. The goal of this work is to utilize this collaboration between casting and AM technologies to show that direct manufacturing of topologically optimized components is possible.

2.4.1 3D Sand Printing

A more direct influence of AM technologies on casting is the recent development of 3D sand printing machines. This process works similar to SLS except that the powder medium is chemically bonded rather than thermally fused; each layer is formed by selectively applying binder to a thin layer of sand. The next layer of sand is distributed then followed by binder. This process repeats until the mold is complete. Post-processing consists of excess sand removal. [12] [33]

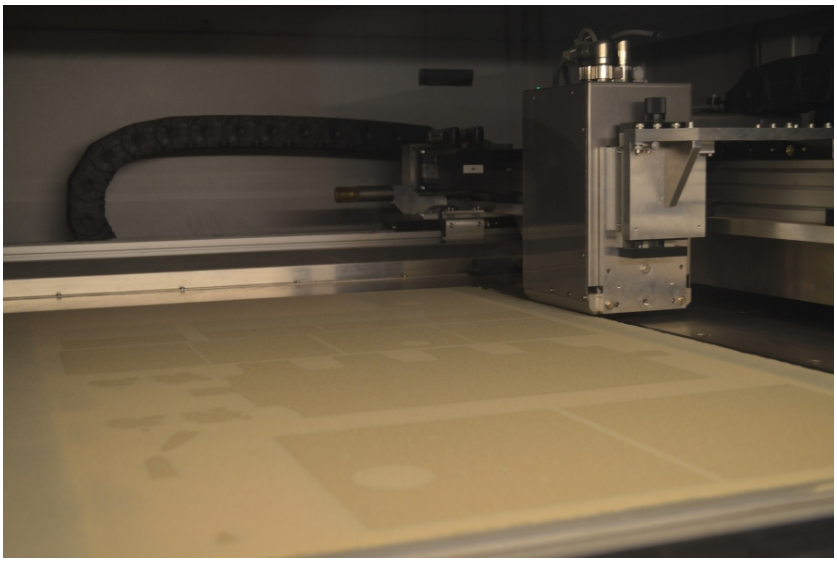

Figure 10: Hetitec's 3D sand printer [34]

Direct printing of the sand molds offers many benefits over traditional sand mold manufacturing methods. One benefit is that printing the mold eliminates the need for a pattern. Printed molds are also more capable; in many cases, they can eliminate the need for separate cores. These sand printers can construct molds with geometry that would be extremely difficult or impossible to create using traditional methods. One benefit from this is the capability to cast a single solid part that would normally consist of an assembly of multiple components. This can reduce or eliminate the stress concentrations often found in fastened, bonded, or welded areas. [35]

Figure 11: Hetitec's demo model, mold, and finished component [34]

Figure 12: 3D printed sand mold core and component [36]

2.5 Topology Optimization and Manufacturing: Current Methods

Topology optimization methods and software have been utilized for component design since the later years of the twentieth century. These optimization tools are used for preliminary structural design then later altered to improve manufacturability. This design alteration usually involves the transformation of complex shapes and features into simpler polygonal geometries. A good example of this design process is shown in Figure 13.

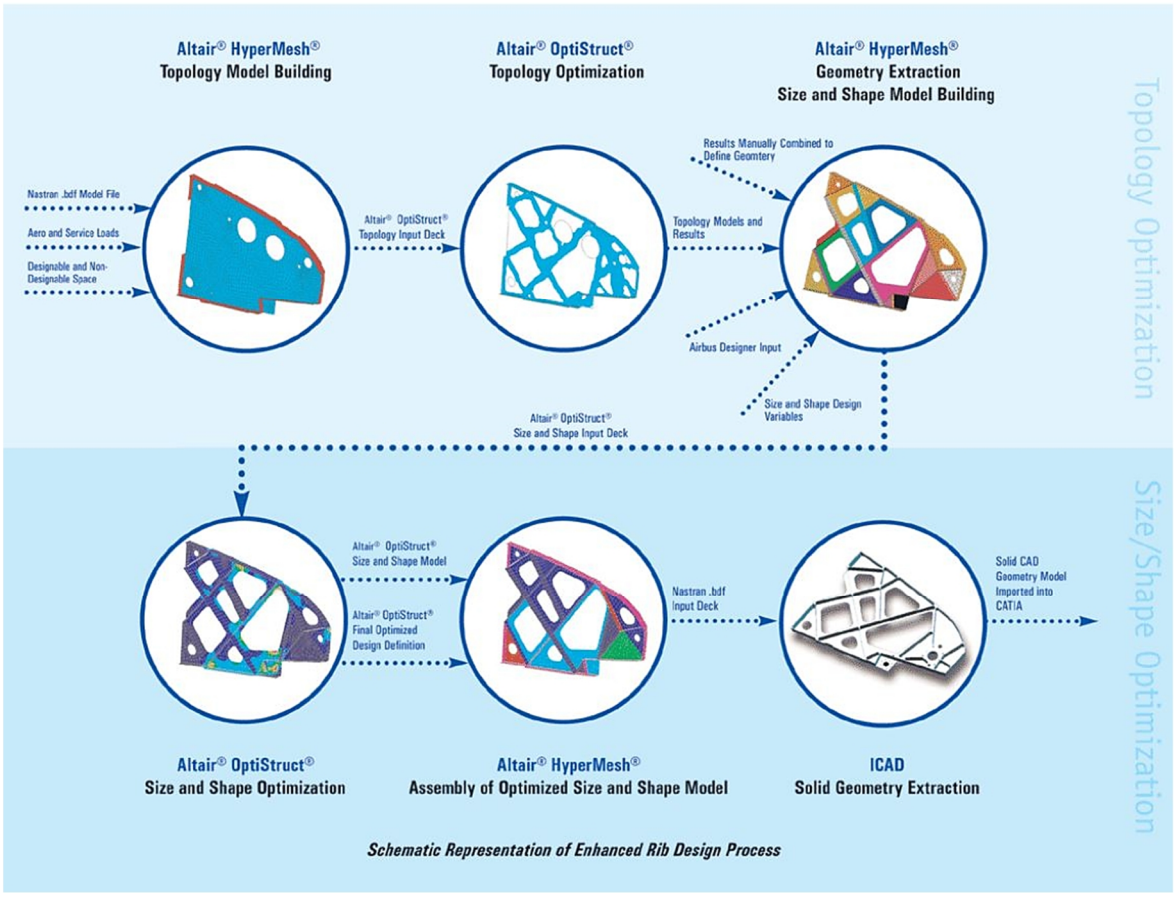

Figure 13: Example of component design process utilizing topology optimization [37]

The direct manufacturing of topologically optimized designs is not currently practiced by any industry. This is because fabricating these optimized designs is costly, timely, and difficult (sometimes impossible) using common manufacturing methods such as milling, stamping, forging, or others. Casting these optimized components using traditional methods is also quite difficult since pattern fabrication usually relies on the manufacturing methods previously mentioned. However, this problem may be resolved if the pattern (or mold) is fabricated using AM technologies.

The emergence of accurate commercialized additive manufacturing technologies provided the first plausible method for the direct manufacturing of topologically optimized components. However, the material selection offered when using AM machinery is limited. Stereolithography and FDM technologies, for example, are limited mainly to resins, polymers, and waxes[4].

Selective laser sintering printers have allowed the direct manufacturing of topologically optimized components. The main advantage of SLS over other FDM technologies is that the list of available materials includes a small selection of metal alloys. Direct metal printing of

[4] The use of concrete with FDM technologies has been improving and increasing, though the application of this material is less-accurate, large-scale, and used mainly for architecture and building construction. [41]

topologically optimized components has proven very useful for RP, testing, and low-volume production. However, using SLS as a mass manufacturing method is not currently plausible due to the high cost, long lead-time, and limited metal alloy selection. [38]

Various technological collaborations have proven beneficial for RP and manufacturing methods. It has been shown that additive manufacturing has allowed the production of topologically optimized components. New casting methods also benefit from AM technologies by allowing the fabrication of highly complex molds. But studies on the collaboration of additive manufacturing, topology optimization, and casting is all but non-existent. This collaboration is explored in this work.

3 Design

3.1 Requirements

High geometric complexity was the primary goal of the design. This complexity is introduced in load-stressed areas where product mass is being limited. The original geometry, desired mass percentage, and load characteristics are the main parameters that determine the resulting geometric intricacy. Although high complexity is desirable, its utility is limited by castability. In this case, the limitations stem from the physical characteristics of molten aluminum. The main limitation addressed during design was wall thickness; any features under 3 mm thick have a higher chance for defects.

Certain aesthetic characteristics were also desired. One of these characteristics was the natural and organic appearance that often occurs from topology optimization. This type of geometry usually resulted without additional effort, though finer details could be manipulated in post-processing using either Inspire or any applicable CAD program.

3.2 Approach

Many initial designs were created using SolidWorks since the outcome of the topology optimization is difficult to predict. These products were designed in order of complexity, starting with simple geometry and loading. The complexity of these parameters were increased with each subsequent design. The design and loading criteria are shown below.

- 2D design with unidirectional 2D loads
- 2D design with multidirectional 2D loads
- 3D design with unidirectional 2D loads
- 3D design with multidirectional 2D loads
- 3D design with multidirectional 3D loads

This design approach helped to understand how Inspire reacted to parameter adjustments and how initial design complexity affected the resulting topology optimization. This order of design also helped identify the optimal level of geometric complexity of the initial design.

Component size was also considered. The ability for a person to be able to hold and observe the product was desired, so keeping the volume and mass relatively low was also important. There was also a limit on how small components can be in order to avoid complications when casting. The ideal size of each design was to fit within a 300 mm cube.

Design recognition was also considered. The resulting goal was to make some designs that were based on real products and some that were completely original. This approach provided the most eclectic collection of designs. The wide range of options also allowed an optimal geometry/load relation for every scenario. An A-arm suspension member is a good example of the more complex side of the design spectrum. It is a very recognizable and intricate (often asymmetrical) component that experiences loads in many different directions and magnitudes. The opposite scenario would be a generic 2D symmetric bracket in tension.

Having such a wide range of designs allowed the development of many different optimized components.

3.2.1 Topology Optimization Software

The optimization software used was Inspire by solidThinking. Three-dimensional CAD models were created in SolidWorks as solid part (.sldprt) files. These files can be imported directly to Inspire. Solid models can be created directly in Inspire but the interface and design capabilities were unfamiliar and basic. The following features and parameters must be defined before Inspire can optimize the model: supports, loads, partitions, material, and design space. Loads are defined by location, direction, and magnitude. There are also load-type options such as point loads, surface loads, and moment loads. Defining a support only requires a location (of a feature) and makes the feature immobile. Partitions geometric features that will not be optimized and are typically areas that are loaded or that act as supports. The design space is all of the geometry that is not a partition.

Some of the most common features that experience loading are holes. For this reason, most of the models were designed with multiple holes (partitioned later as hollow cylinders) acting as pre-determined force/support locations. This worked well during optimization and also has relevance to real-world applications. All of the partition features have very defined edges that can be rounded or chamfered later for improved aesthetics and castability.

3.3 Component Designs

The design goal for this work was to create objects with geometries that were complex, aesthetically pleasing, and difficult to cast using common methods. A minimum of two designs needed to meet these standards. This would allow one product to be investment cast and the other to be cast with a 3D printed sand mold. Many designs and design iterations were created in order to maximize geometric variation. This allowed the optimal choices for both casting methods.

3.3.1 Simple Brackets

Three generic brackets represented the simplest designs with the most basic loading scenarios. These brackets are listed below.

- Triangular bracket – This was an equilateral triangular plate bracket with a hole at each vertex. It was subjected to various tension forces along the plate plane. The optimization results did not yield any complex geometry (can be seen in Figure 51).
- Box bracket – This was a 3D model having the basic dimensions of a cube. The model was subjected to simple compression forces on two opposing sides. The topology optimization yielded geometry with low complexity.
- Anchor bracket – This design was more complex due to the presence of five different holes. This allowed many combinations of load directions and magnitudes. The two best results (Figure 14) only differed by one load; one in the positive X-direction on the top hole.

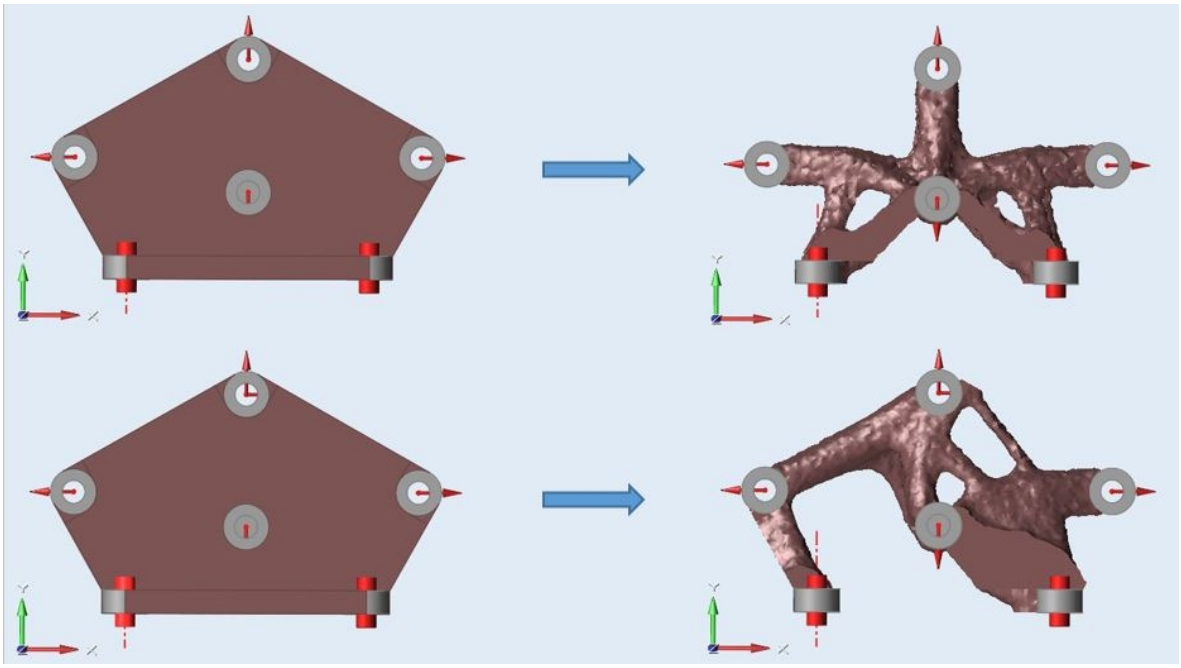

Figure 14: Anchor bracket topology optimizations with different load cases

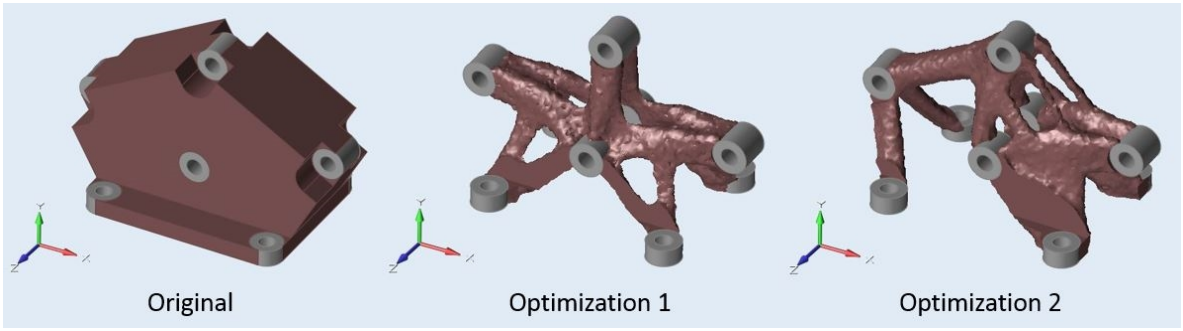

Figure 15: Anchor brackets iso view

3.3.2 Support Beam

The support beam was a custom design based off a square tube with two end supports and one central load. The end supports, surfaces were perpendicular to each other (Figure 16) and the central load was simulated as a hanging weight (-y direction). This was a 3D design with 2D loadings. Some desirable 3D geometries resulted, varying with changes to the magnitude and direction of loadings and to target mass percentage.

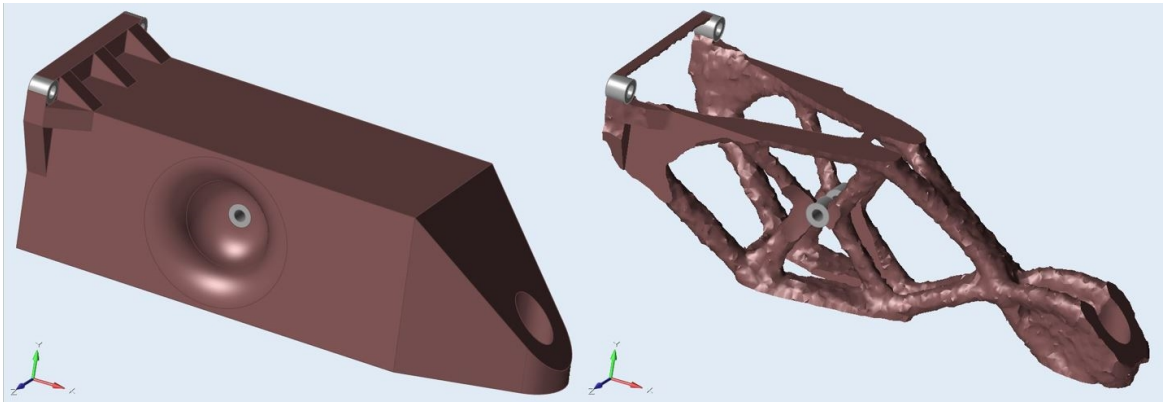

Figure 16: Support beam

3.3.3 Brake Pedal

The brake pedal design was the first attempt at recreating a recognizable product. It was modeled as a generic automobile brake pedal with two holes (one as a rotation point and one as a load point) and a square surface (that was assigned a pressure force) to represent the pedal. The original body of the pedal was designed out of a plate of relatively low thickness. This geometry, and the applied loadings, essentially made it a 2D object with 2D loadings. Surprisingly, the topology optimization results yielded some 3D geometries. This can be seen near the bottom of the body (Figure 17) near the pedal. These results prompted further design development by using the polyNURBS tool found in Inspire.

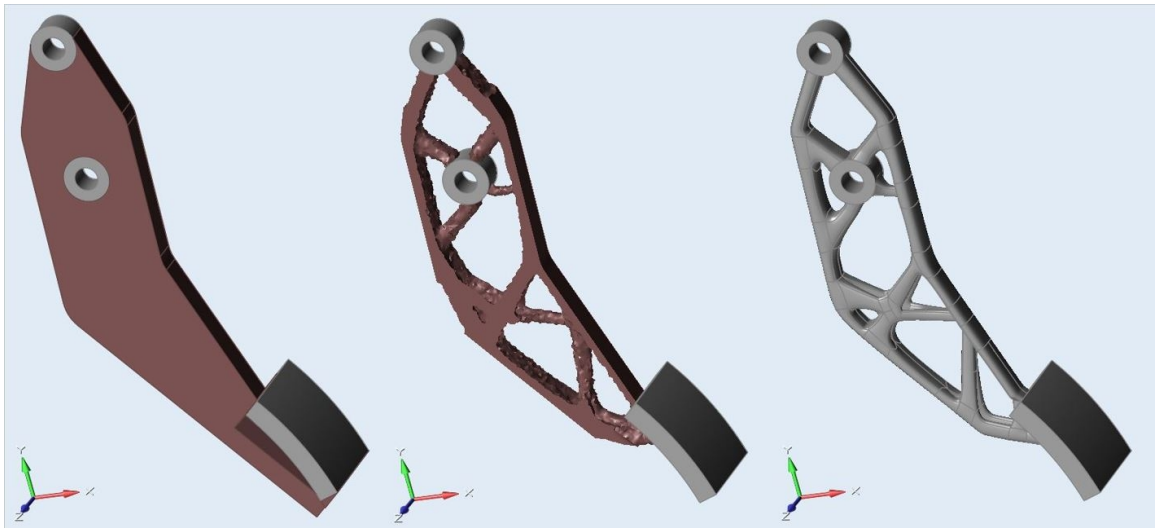

Figure 17: Brake pedal at different stages (original, optimized, polyNURBS)

3.3.4 Steering Knuckle

The steering knuckle design was also based off those found on various vehicles. Steering knuckles can vary greatly depending on the application, so the model in this work was a generic design. This was a 3D design with 3D loadings. Support and loading parameters were defined according to what a typical steering knuckle might experience. The best optimization results were achieved with a 20% target mass. The results from the topology

optimization fit well with the design goals; the object had geometries that were complex and aesthetically pleasing. The component would also be difficult to cast using common methods due to the need for multiple complex cores. The steering knuckle design was further developed using polyNURBS.

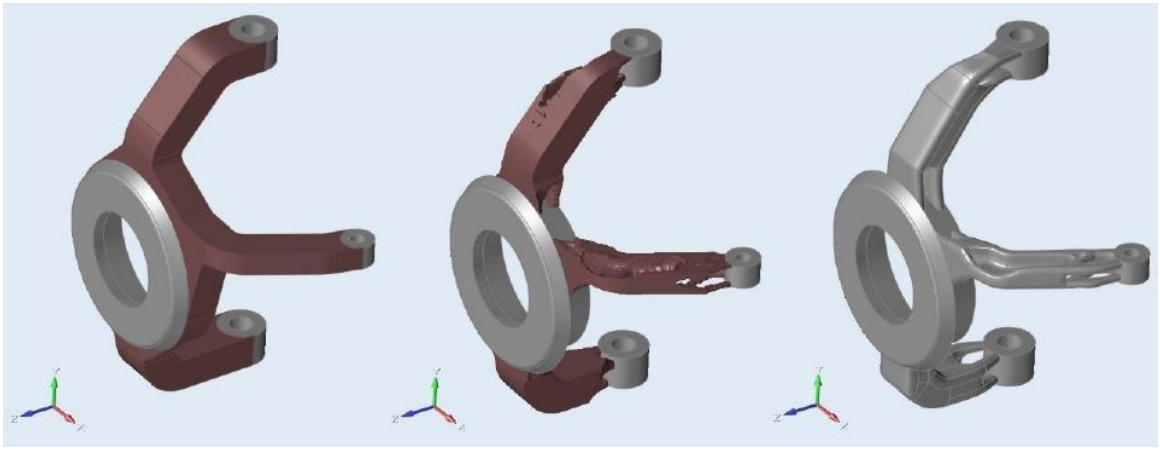

Figure 18: Steering knuckle at different stages (original, optimized, polyNURBS)

3.3.5 Propeller Hub

The propeller hub design was loosely based off those that are found on helicopters. A 4-propeller design was chosen due to desirable symmetry and ease of load application; a 4-propeller design aligns perfectly with the coordinate system (and planes) of 3D modeling programs. This was a 3D design with 3D loadings. Support and loading parameters were defined according to what a typical helicopter propeller hub might experience. The best optimization results were achieved with a 15% target mass. The geometries resulting from the topology optimization of this model also fulfilled the design goals adequately. The propeller hub design was further developed using polyNURBS and then prepared for casting.

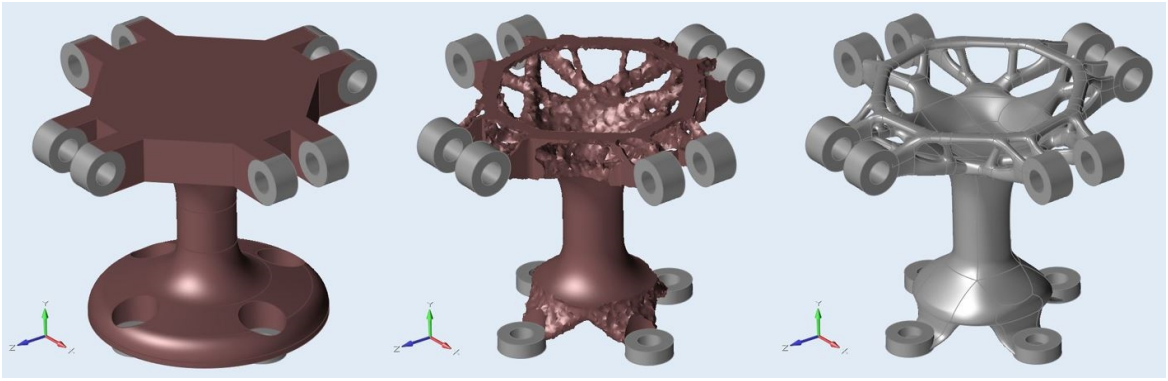

Figure 19: Propeller hub at different stages (original, optimized, polyNURBS)

3.3.6 Lower A-arm

The lower A-arm was another design that was based off a real product that, in this case, is a vehicle suspension system component. This was a 3D design with 3D loadings. Support and loading parameters were defined according to what a typical lower A-arm might experience. The best optimization results were achieved with a 15% target mass. The topology optimization resulted in some intricate geometries and was still recognizable as a real-life product. The model was further developed using polyNURBS and then prepared for casting.

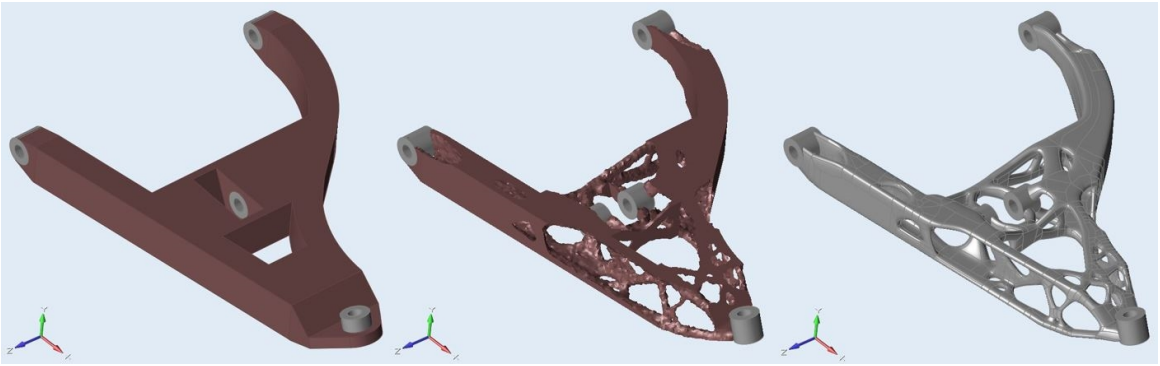

Figure 20: Lower A-arm at different stages (original, optimized, polyNURBS)

3.4 Selected Designs

The two designs selected for casting were the propeller hub and the lower A-arm. The propeller hub was chosen for investment casting while the lower A-arm was chosen for casting in a 3D printed sand mold provided by Hetitec. Hetitec is a 3D printing company based near Tampere, Finland. They provide 3D printed sand molds to many leading Scandinavian companies in the mechanical engineering industry. The company establishes their vision on their website's home page with "Hetitec is specialized in on-demand production of moulds and models for metal casting via 3D printing. The more complicated the part and tighter the schedule, the more competitive Hetitec 3D printing method is compared to the traditional tooling-based mould manufacturing methods." [34]

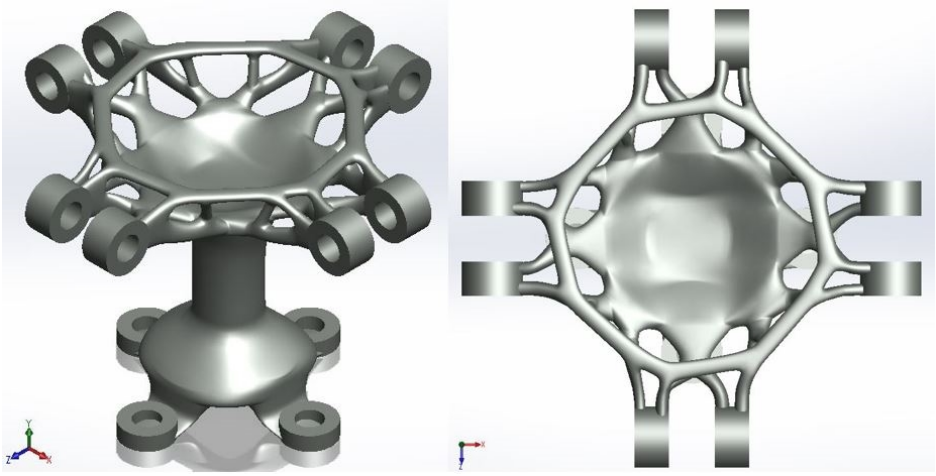

Figure 21: Propeller hub iso and top (.step model in SolidWorks)

The investment casting mold was formed over a 3D printed wax pattern of the propeller hub. This was accomplished on campus using Aalto University's new 3D wax printer. These two models were selected because they provided the best balance of intricacy, castability, and product familiarity. The propeller hub was a great candidate for IC because of its small scale and good 3D printability (for the consumable wax pattern). A 3D printing of the lower A-arm was less desirable because of its larger size and because it would require a high volume of support material. These factors made the lower A-arm a better fit for 3D printed sand mold casting.

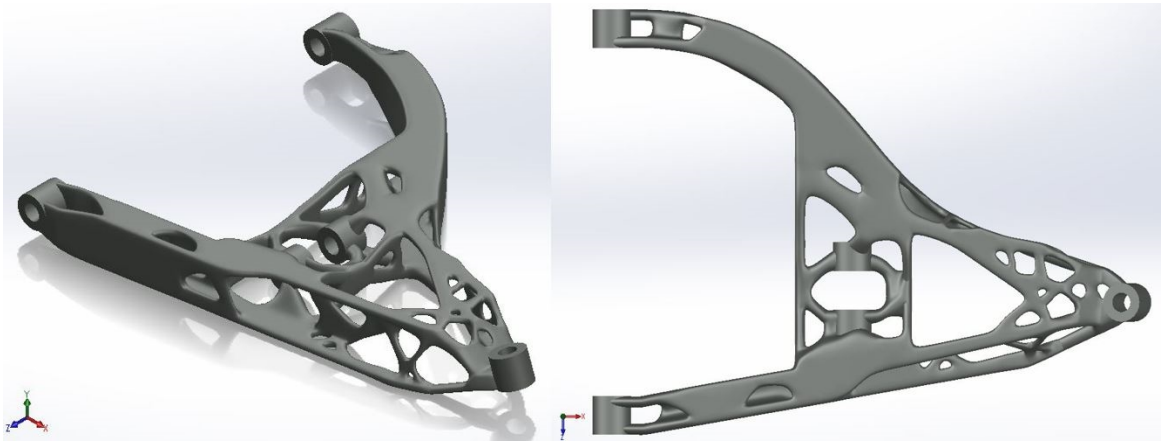

Figure 22: Lower A-arm iso and top (.step model in SolidWorks)

4 Simulations

Casting simulations were accomplished using Magma5.3 for both casting processes. Various simulations were done for each of the two components in order to analyze flow, cooling, solidification, and porosity characteristics. These simulations were performed in order gain a better insight towards the type of, and severity of, modifications that would be needed in order to optimize the casting process[5].

4.1 Propeller Hub

Some general parameters had to be established before running the simulations (Table 1). The mold is simulated with a preheated temperature and the simulated material is the same as the component material.

Table 1: Propeller Hub Simulation Parameters

Mold Temperature	450°C
Pour Temperature	740°C
Pour Duration	4 seconds
Material	AlSi10

The snapshots below in Figure 23 show the molten flow path and velocities. Once the melt reaches the propeller hub portion the flow is uniform with minimal turbulence.

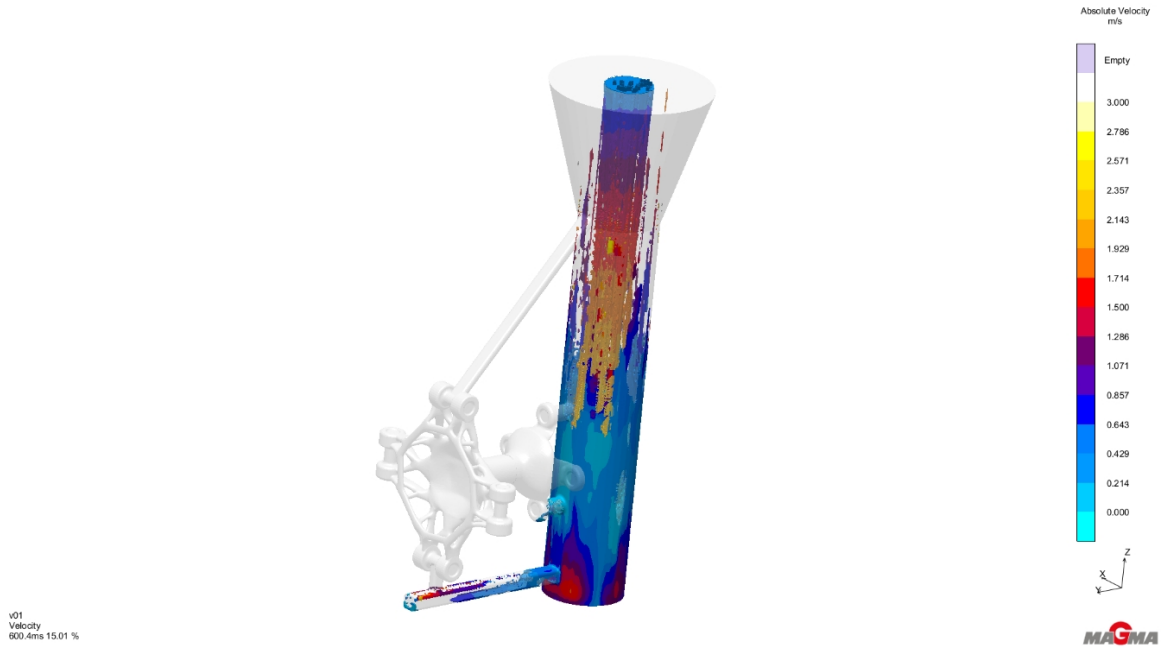

(a)

[5] The simulations were *only for insight*; optimizing the casting process could be a thesis on its own.

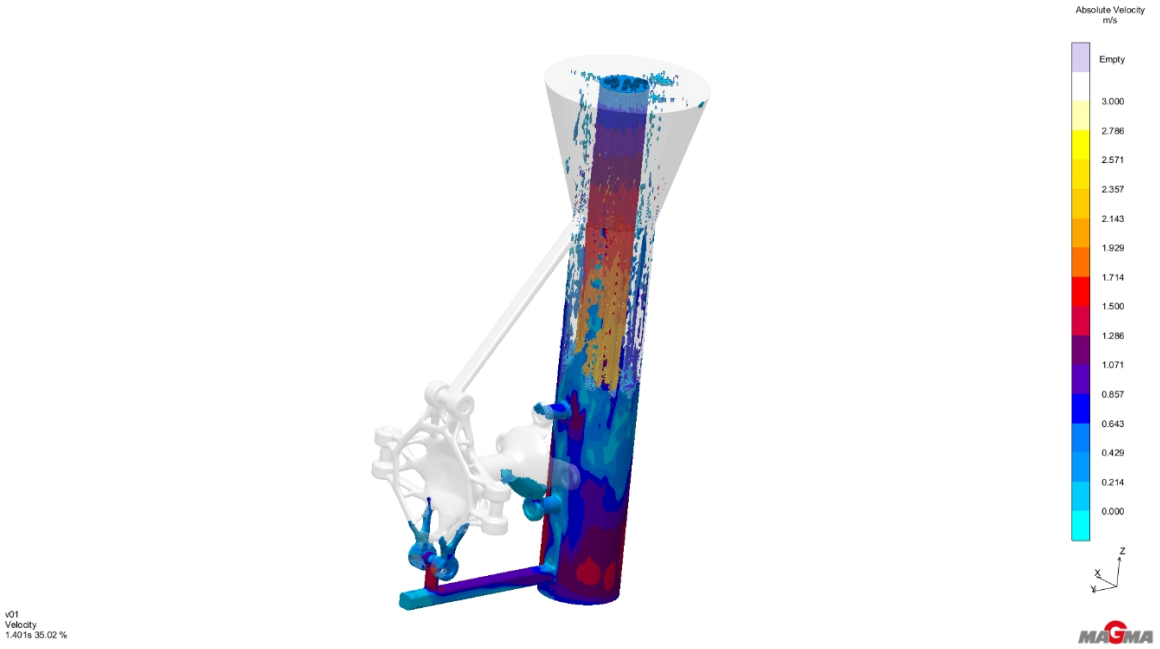
Absolute Velocity
m/s
Empty
3.000
2.786
2.571
2.357
2.143
1.929
1.714
1.500
1.286
1.071
0.857
0.643
0.429
0.214
0.000
Z
X
Y
MAGMA
v01
Velocity
1.401s 35.02 %

(b)

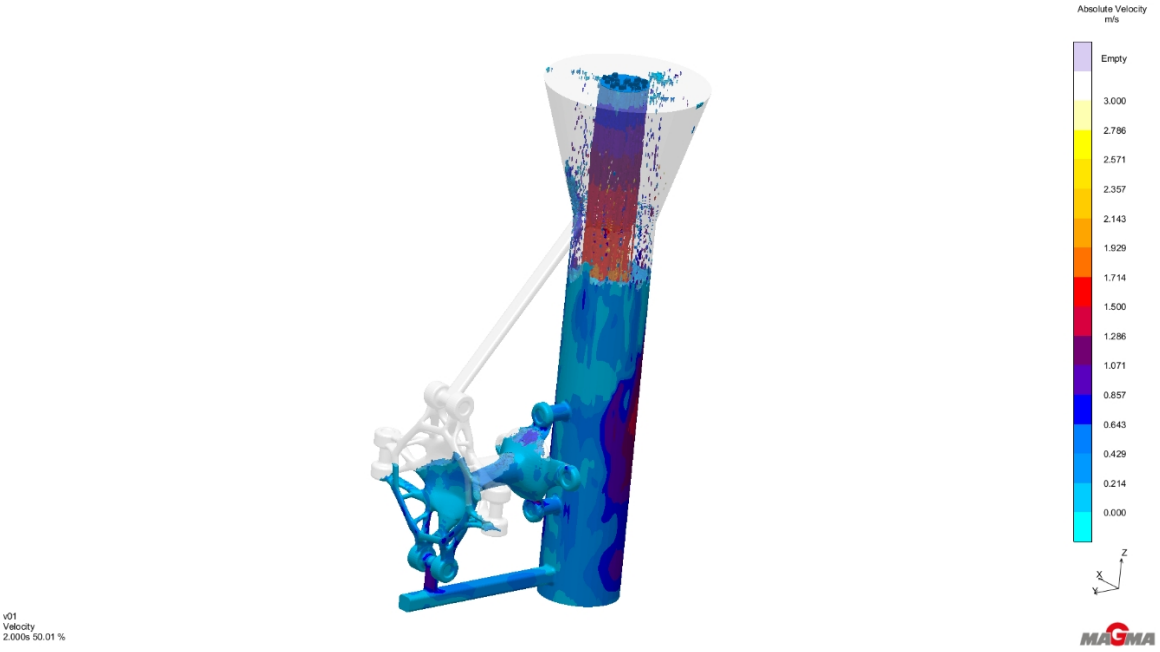
Absolute Velocity
m/s
Empty
3.000
2.786
2.571
2.357
2.143
1.929
1.714
1.500
1.286
1.071
0.857
0.643
0.429
0.214
0.000
Z
X
Y
MAGMA
v01
Velocity
2.000s 50.01 %

(c)

(d)

Figure 23: Time lapse of molten flow velocities in the propeller hub mold

The snapshots below in Figure 24 show the molten flow temperatures. The results of the cooling conditions are also quite nice. The component area cools evenly, gradually, and without the presence of drastic hot or cold spots.

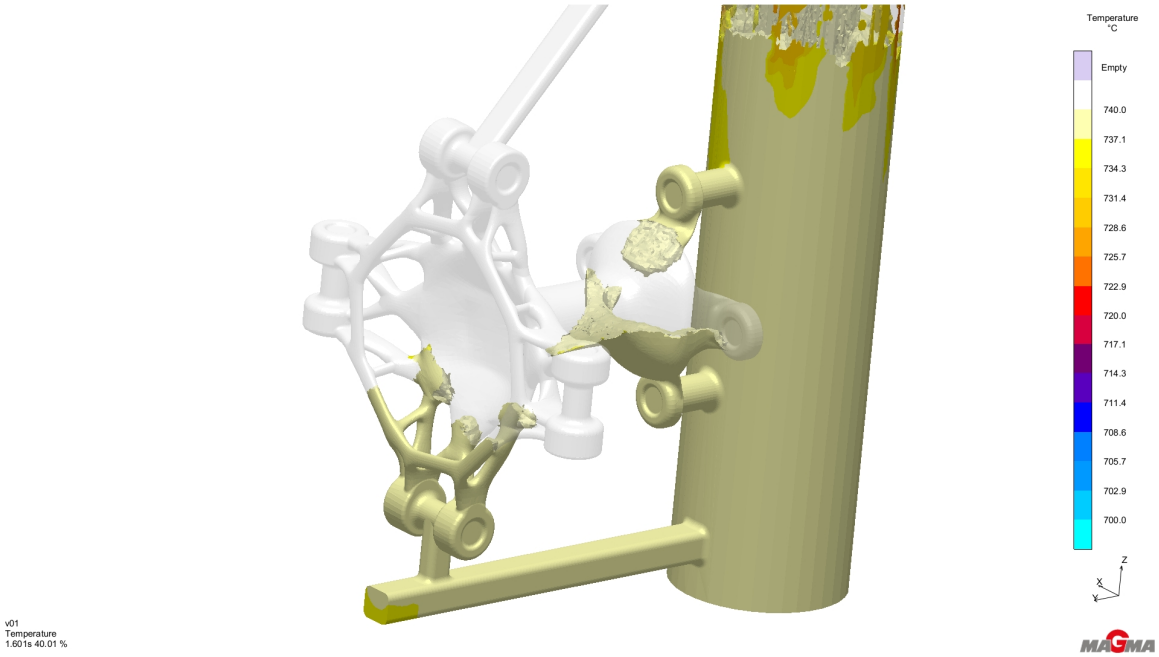

(a)

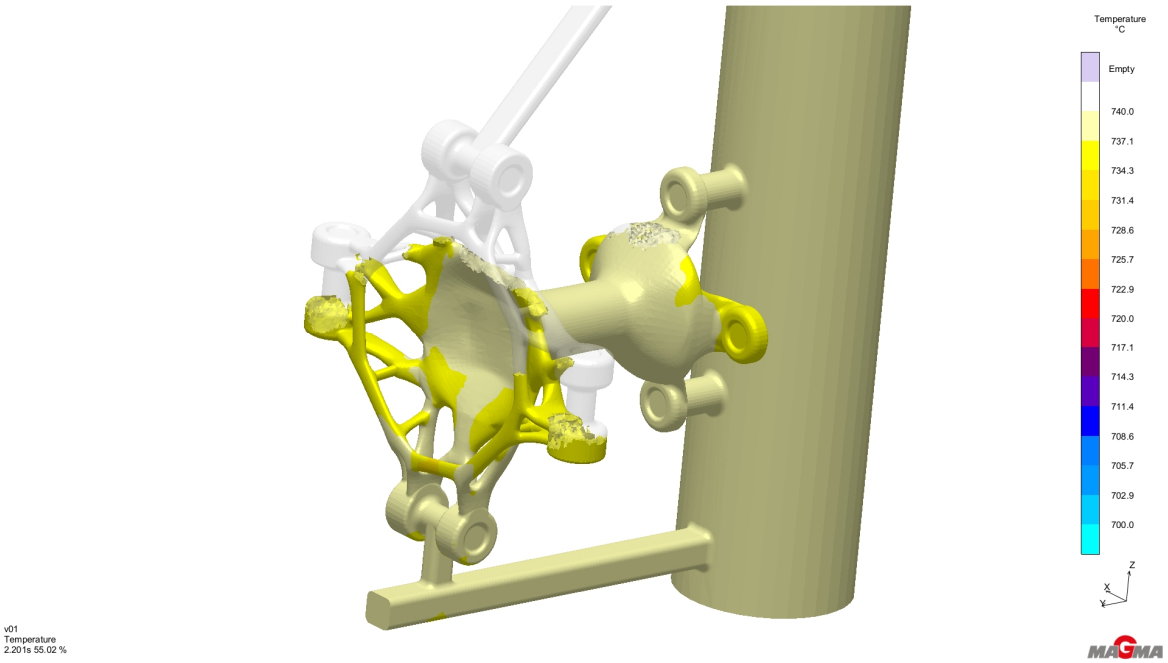
Temperature
°C
Empty
740.0
737.1
734.3
731.4
728.6
725.7
722.9
720.0
717.1
714.3
711.4
708.6
705.7
702.9
700.0
Z
X
Y
v01
Temperature
2.201s 55.02 %
MAGMA

(b)

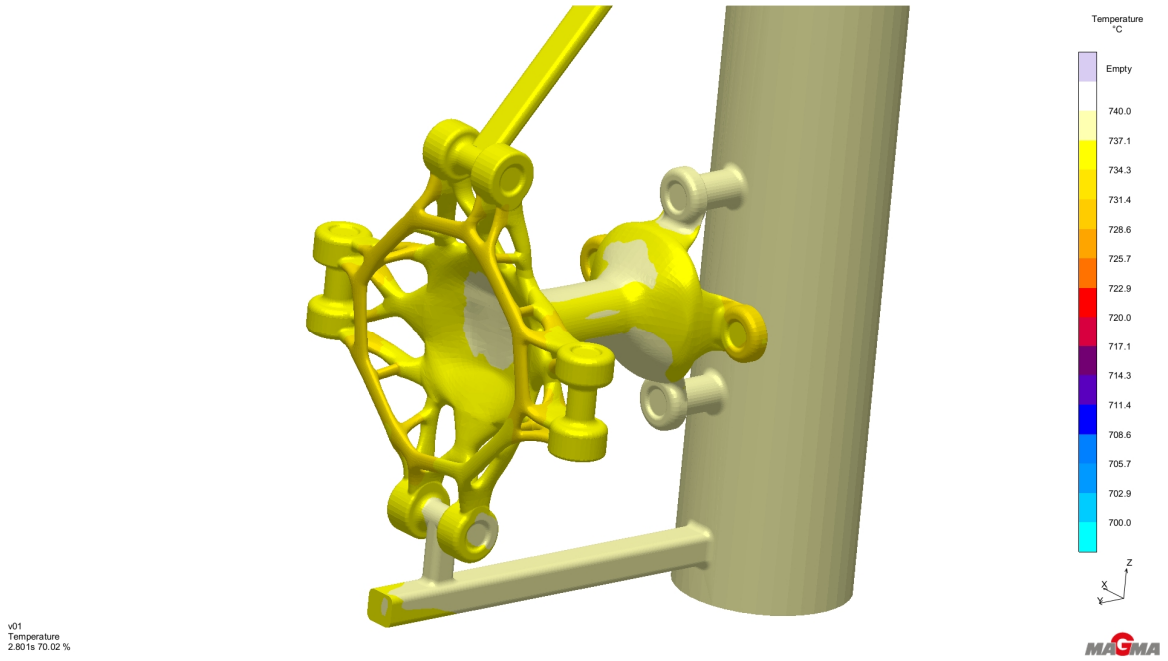
Temperature
°C
Empty
740.0
737.1
734.3
731.4
728.6
725.7
722.9
720.0
717.1
714.3
711.4
708.6
705.7
702.9
700.0
Z
X
Y
v01
Temperature
2.801s 70.02 %
MAGMA

(c)

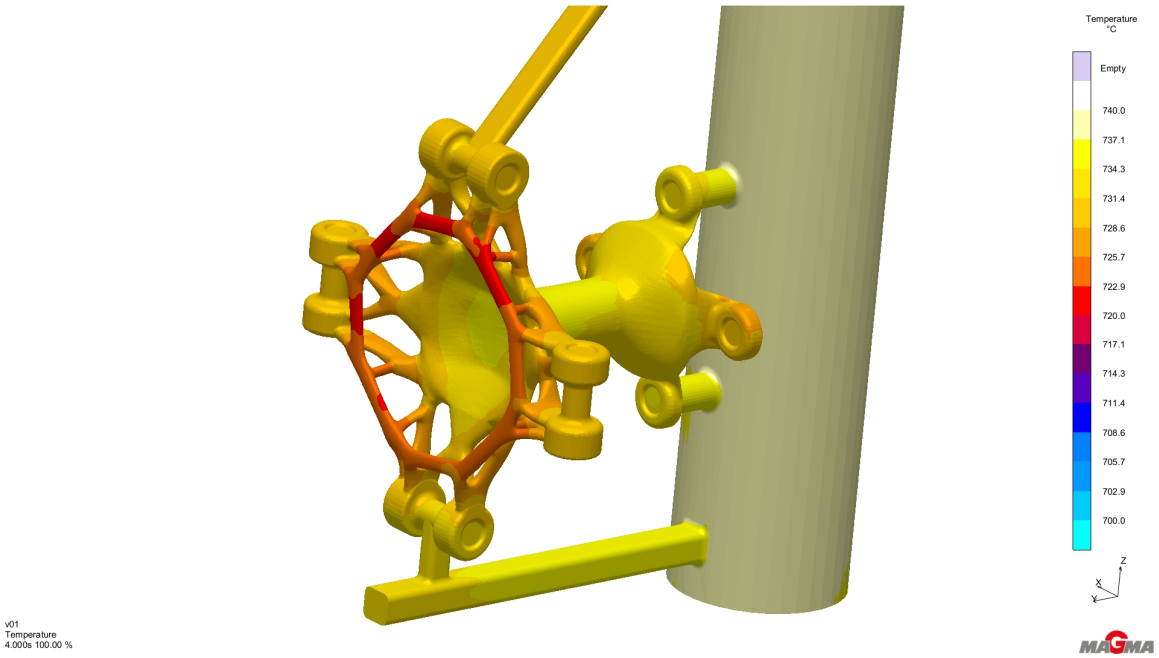

(d)

Figure 24: Time lapse of molten flow temperatures in the propeller hub mold

The snapshots below in Figure 25 show the solidification characteristics. Solidification occurs in multiple isolated areas during the cooling process due to the great size differences between adjacent bodies. Localized premature cooling may lead to some internal stresses and possibly cracking.

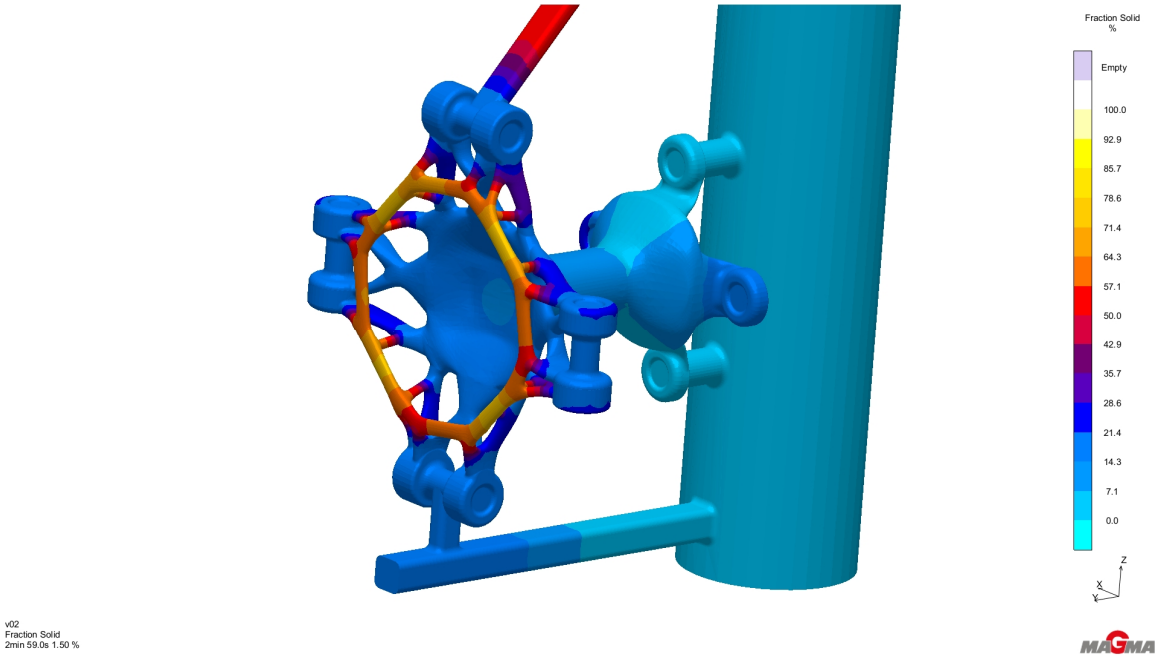

(a)

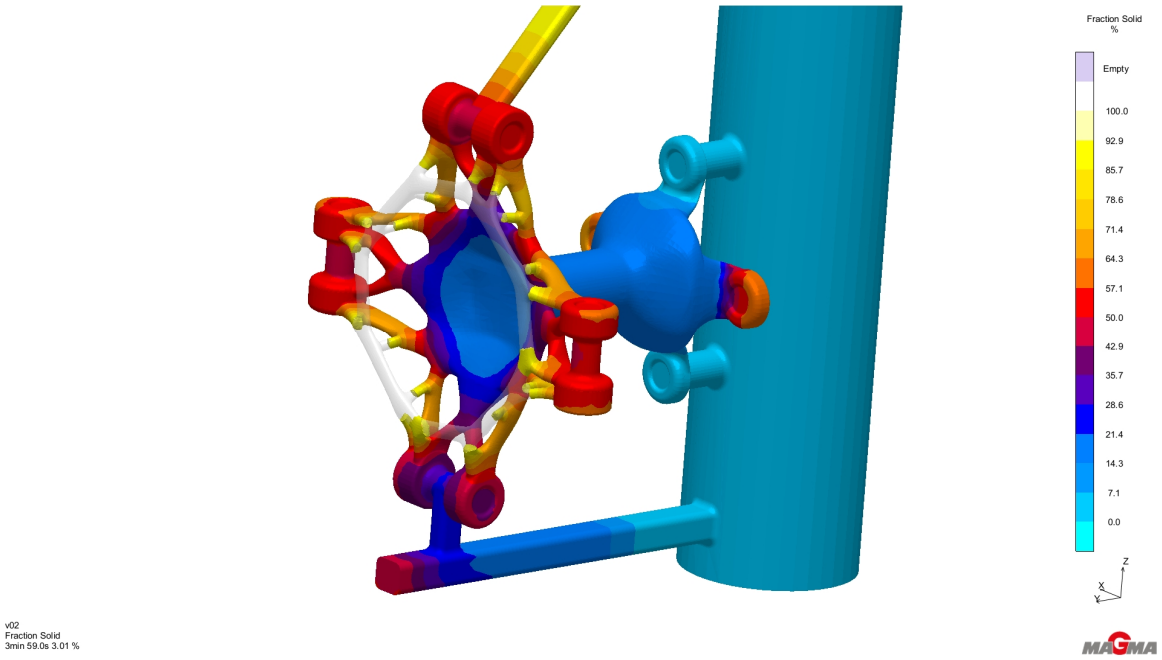
Fraction Solid
%
Empty
100.0
92.9
85.7
78.6
71.4
64.3
57.1
50.0
42.9
35.7
28.6
21.4
14.3
7.1
0.0
Z
X
Y
v02
Fraction Solid
3min 59.0s 3.01 %
MAGMA

(b)

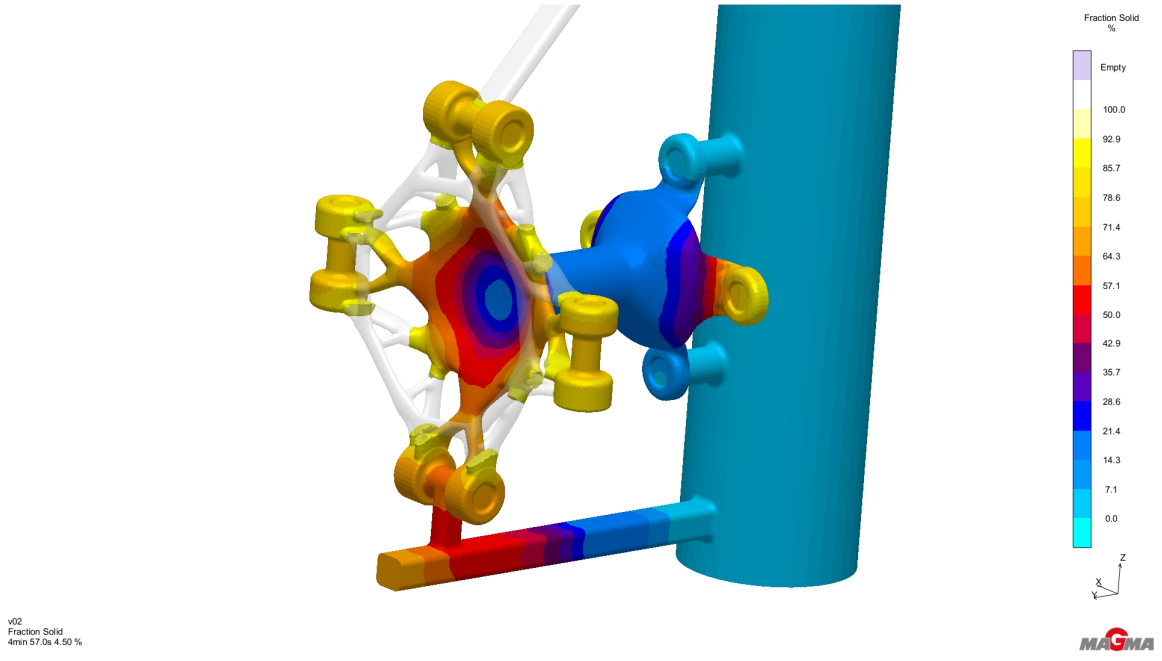
Fraction Solid
%
Empty
100.0
92.9
85.7
78.6
71.4
64.3
57.1
50.0
42.9
35.7
28.6
21.4
14.3
7.1
0.0
Z
X
Y
v02
Fraction Solid
4min 57.0s 4.50 %
MAGMA

(c)

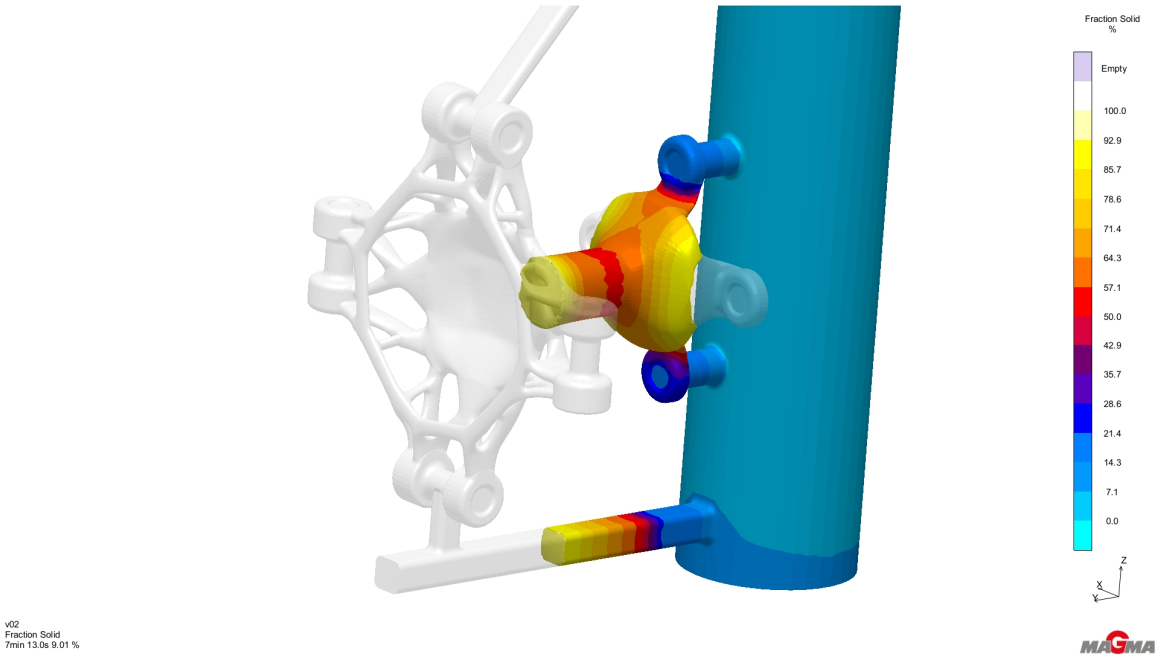

(d)

Figure 25: Time lapse of solidification in the propeller hub mold

The porosity simulation results shown below in Figure 26 are very nice since there are very few porosity locations with very low porosity level.

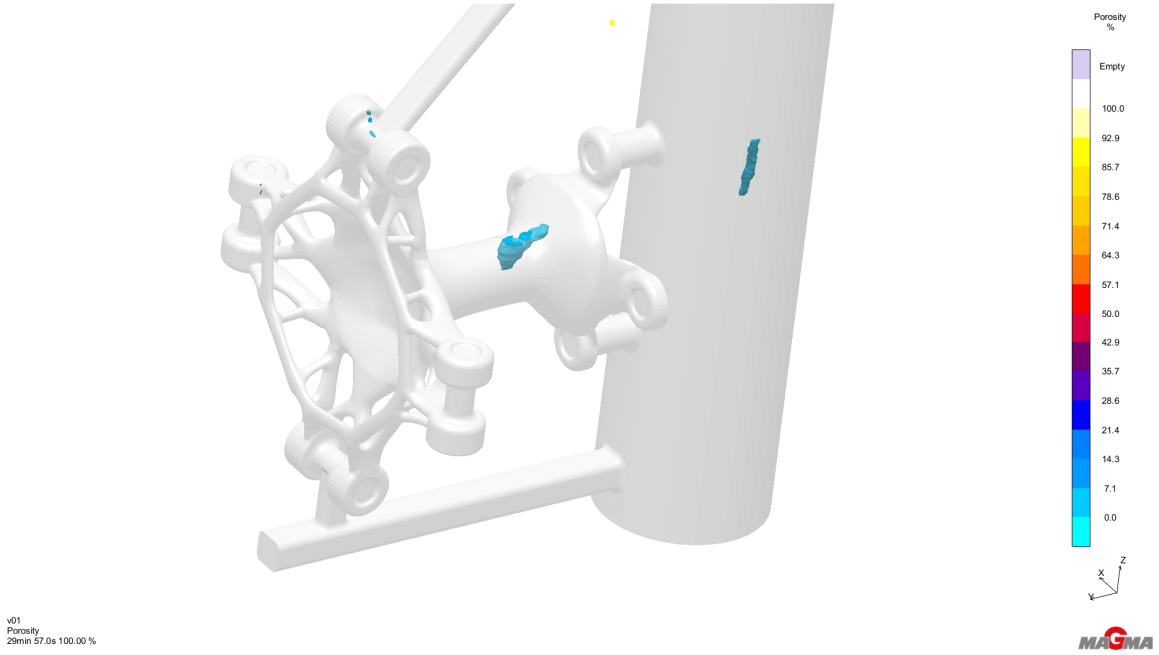

Figure 26: Simulated porosities in the propeller hub

4.2 Lower A-arm

Some general parameters had to be established before running the simulations (Table 2). The mold was not preheated and the simulated material is the same as the component material.

Table 2: Lower A-arm Simulation Parameters

Mold Temperature	20°C
Pour Temperature	740°C
Pour Duration	5 seconds
Material	AlSi10

The snapshots below in Figure 27 show the molten flow path and velocities. The presence of multiple flow fronts, and the collisions between them, may cause problems with the pour. These fronts can be seen well in Figure 27 (b) and (c). Some concentrated high-velocity areas may cause some turbulence but should not cause any major problems.

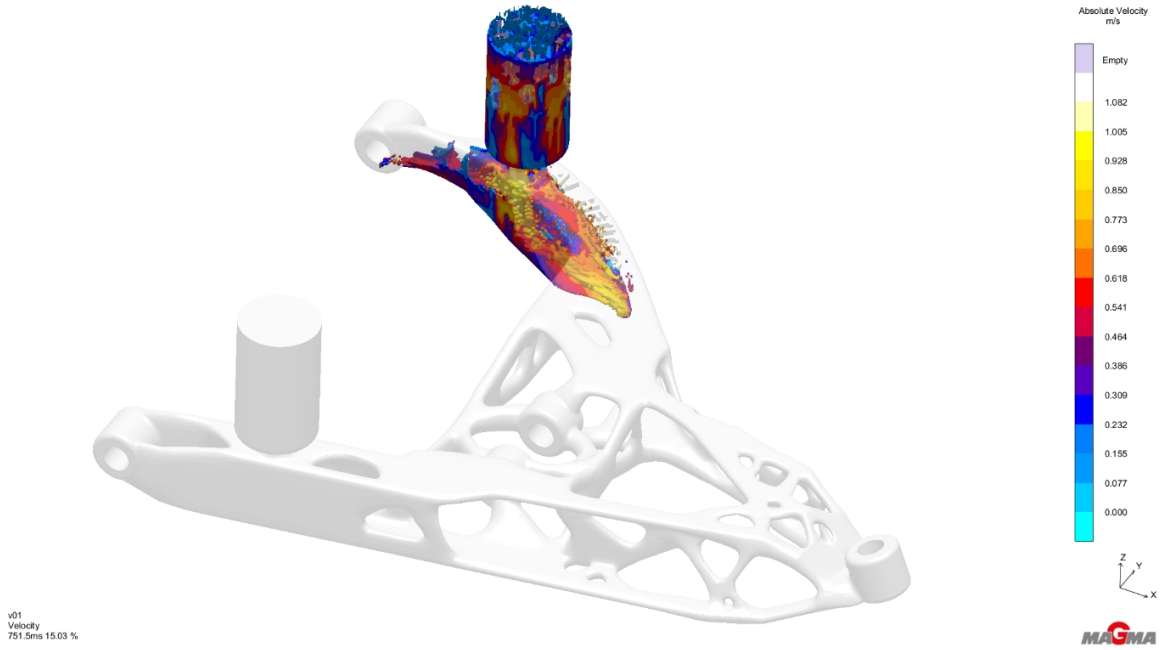

(a)

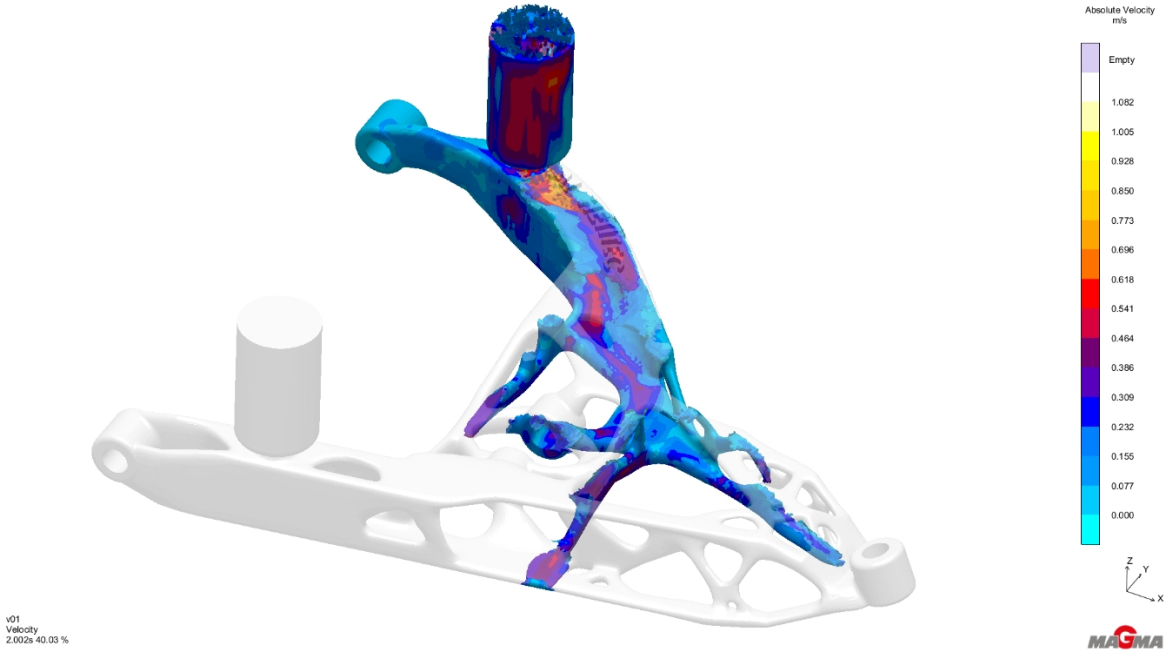
Absolute Velocity
m/s
Empty
1.082
1.005
0.928
0.850
0.773
0.696
0.618
0.541
0.464
0.386
0.309
0.232
0.155
0.077
0.000
Z
Y
X
MAGMA
v01
Velocity
2.002s 40.03 %

(b)

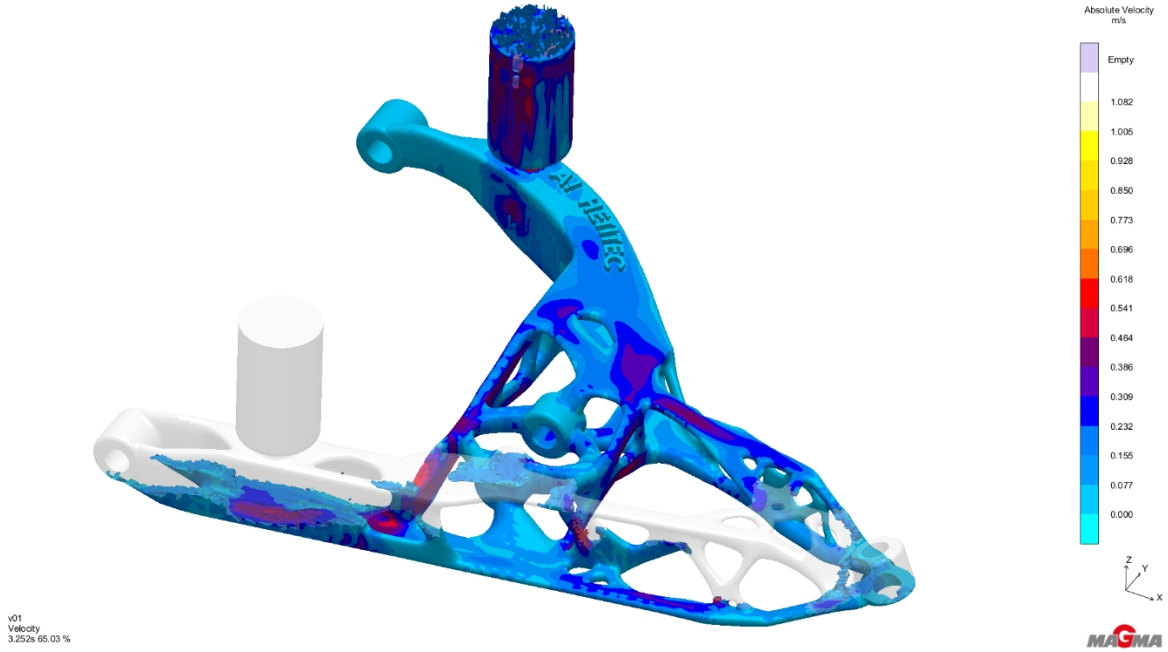
Absolute Velocity
m/s
Empty
1.082
1.005
0.928
0.850
0.773
0.696
0.618
0.541
0.464
0.386
0.309
0.232
0.155
0.077
0.000
Z
Y
X
MAGMA
v01
Velocity
3.252s 65.03 %

(c)

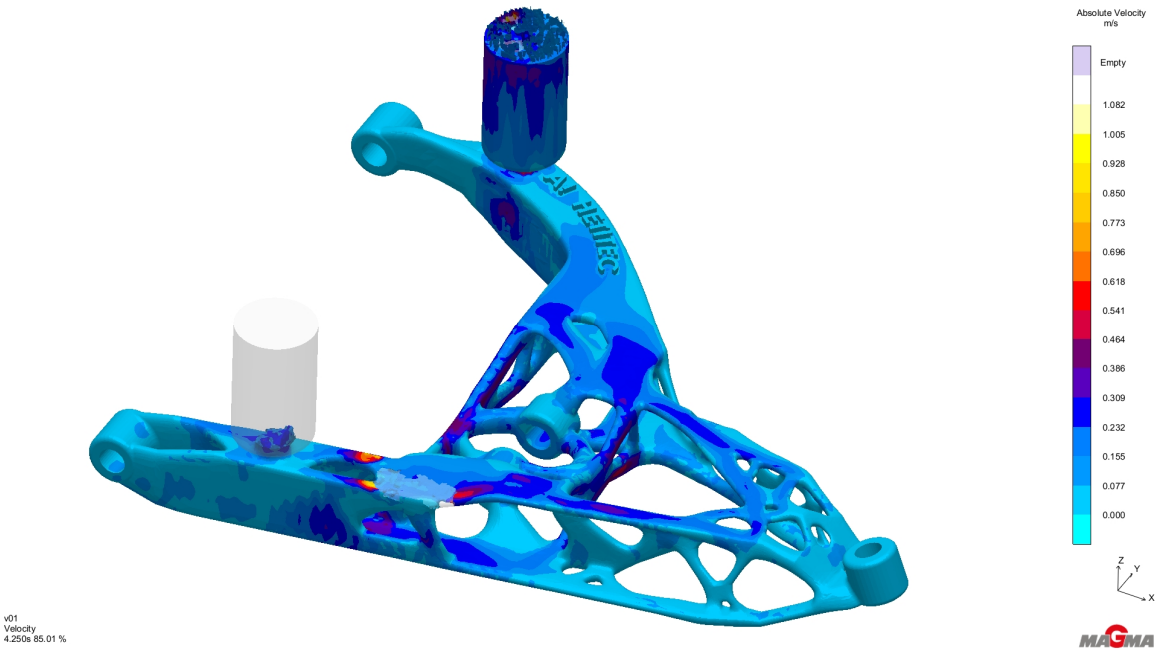

(d)

Figure 27: Time lapse of molten flow velocities in the lower A-arm mold

The snapshots below in Figure 28 show the molten flow temperatures. Most of the possible problem areas are focused at the 'point' (right-most section of the component) of the lower A-arm where rapid cooling occurs. The probable causes of this rapid cooling are listed below.

1. The point of the lower A-arm contains many small diameter and long (in comparison to the diameter) passages.
2. Many flow fronts form in and travel through the point of the lower A-arm.
3. The point of the lower A-arm is one of the further areas from the sprue.

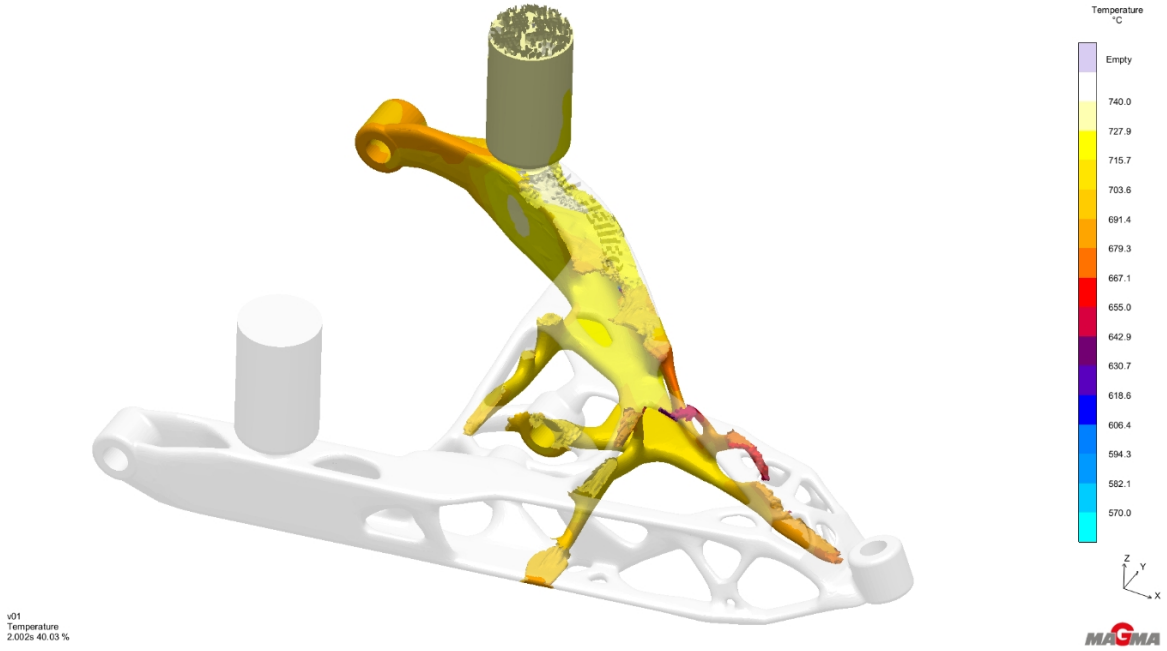
Temperature
°C
Empty
740.0
727.9
715.7
703.6
691.4
679.3
667.1
655.0
642.9
630.7
618.6
606.4
594.3
582.1
570.0
Z
Y
X
MAGMA
v01
Temperature
2.002s 40.03 %

(a)

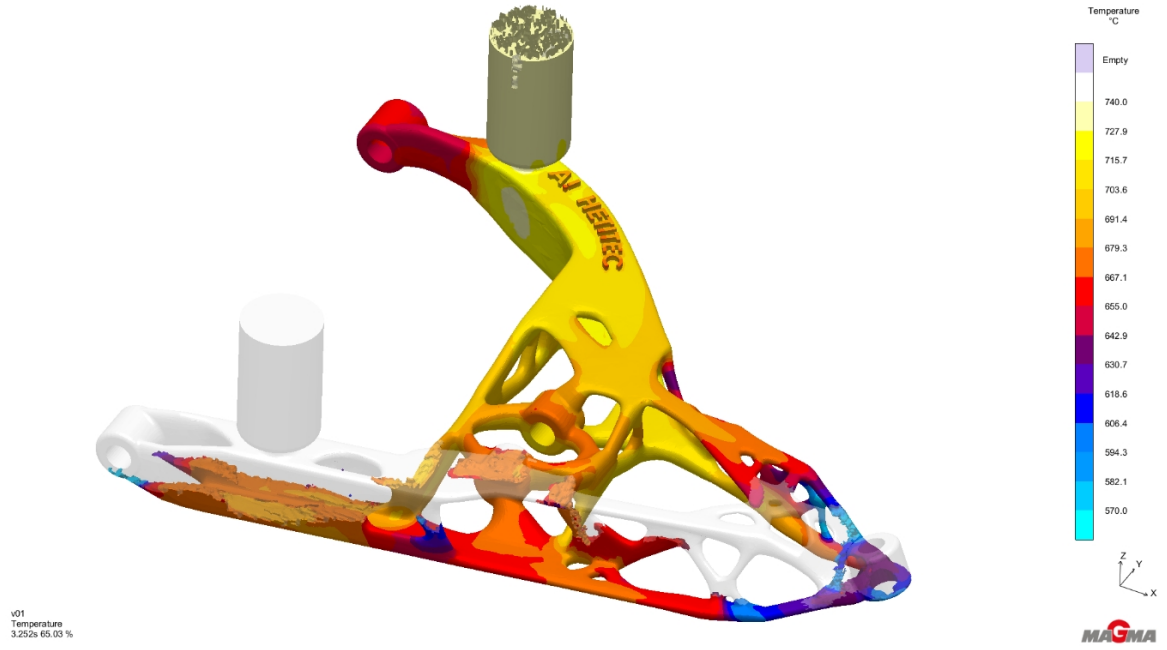
Temperature
°C
Empty
740.0
727.9
715.7
703.6
691.4
679.3
667.1
655.0
642.9
630.7
618.6
606.4
594.3
582.1
570.0
Z
Y
X
MAGMA
v01
Temperature
3.252s 65.03 %

(b)

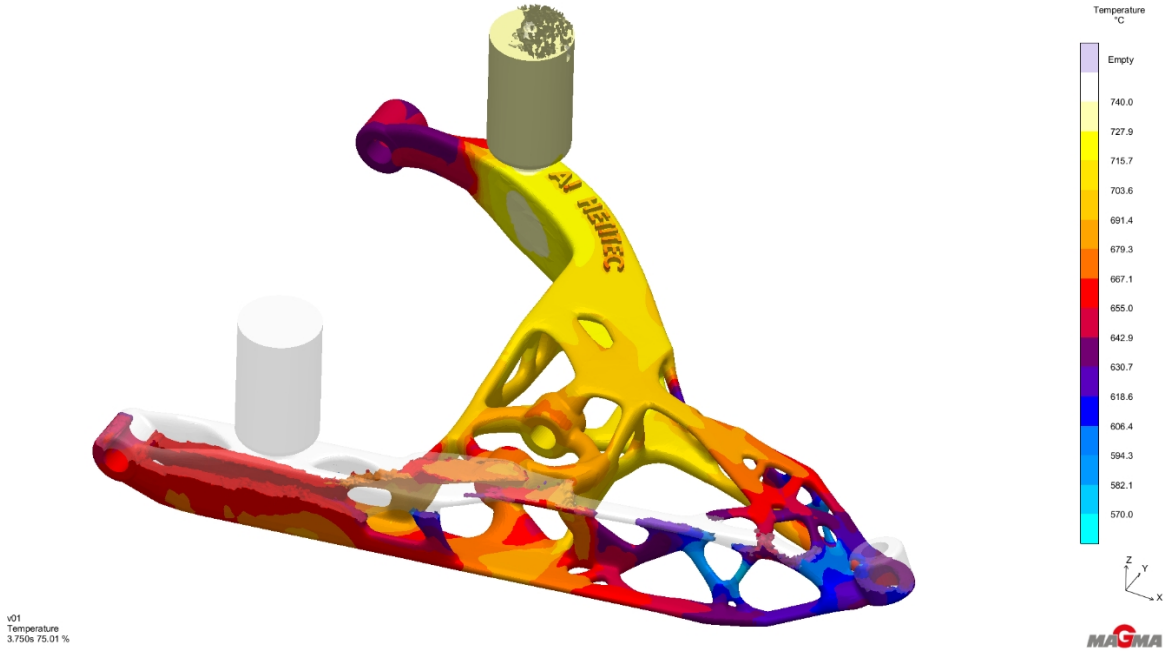

(c)

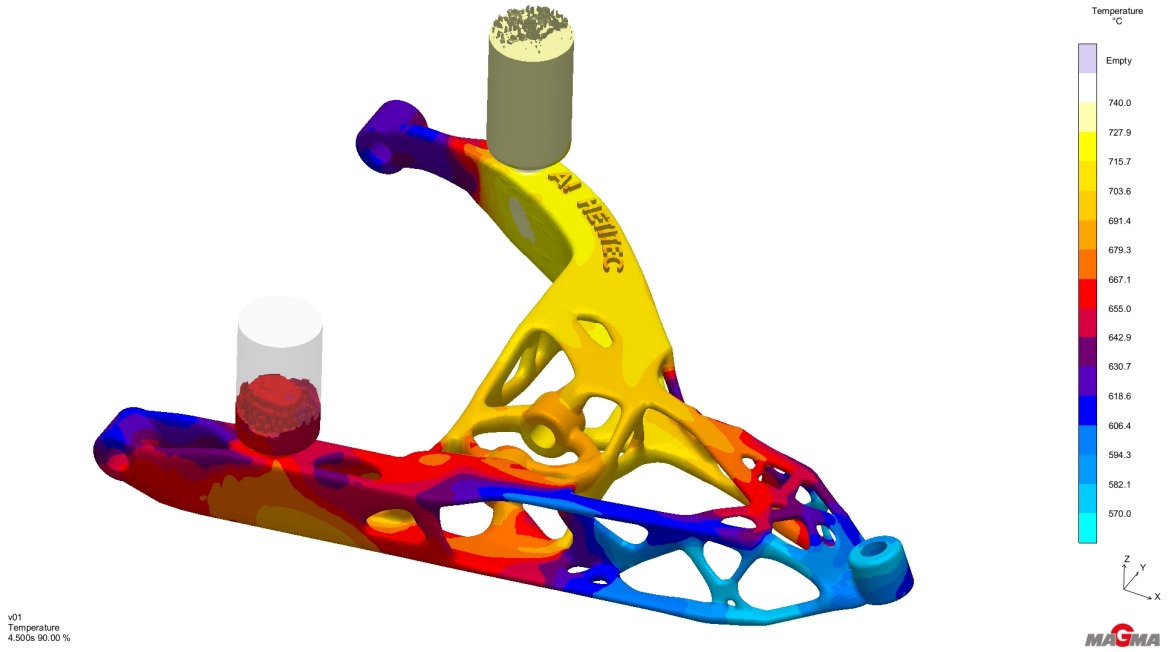

(d)

Figure 28: Time lapse of molten flow temperatures in the lower A-arm mold

The snapshots below in Figure 29 show the solidification characteristics. The isolated hot spots in the tip and center (seen well in Figure 29 (b) and (d)) may cause defects to form. The contraction of these isolated areas causes stresses in adjacent solid bodies, which can lead to cracking and porosity.

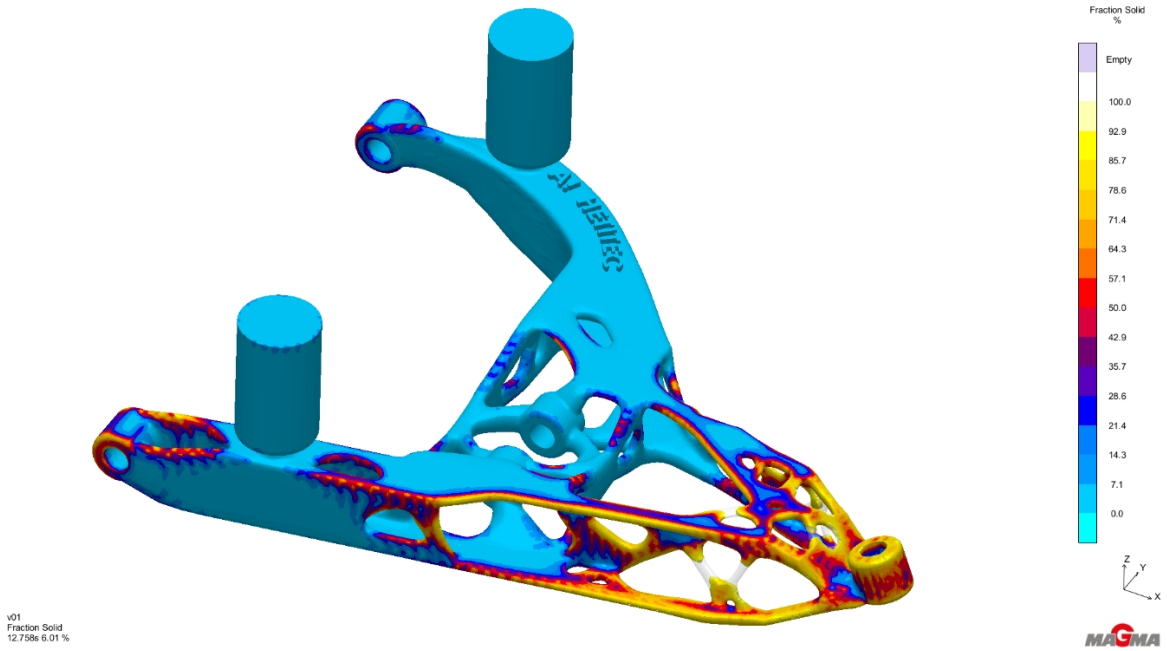
Fraction Solid
%
Empty
100.0
92.9
85.7
78.6
71.4
64.3
57.1
50.0
42.9
35.7
28.6
21.4
14.3
7.1
0.0
Z
Y
X
MAGMA
v01
Fraction Solid
12.758s 6.01 %

(a)

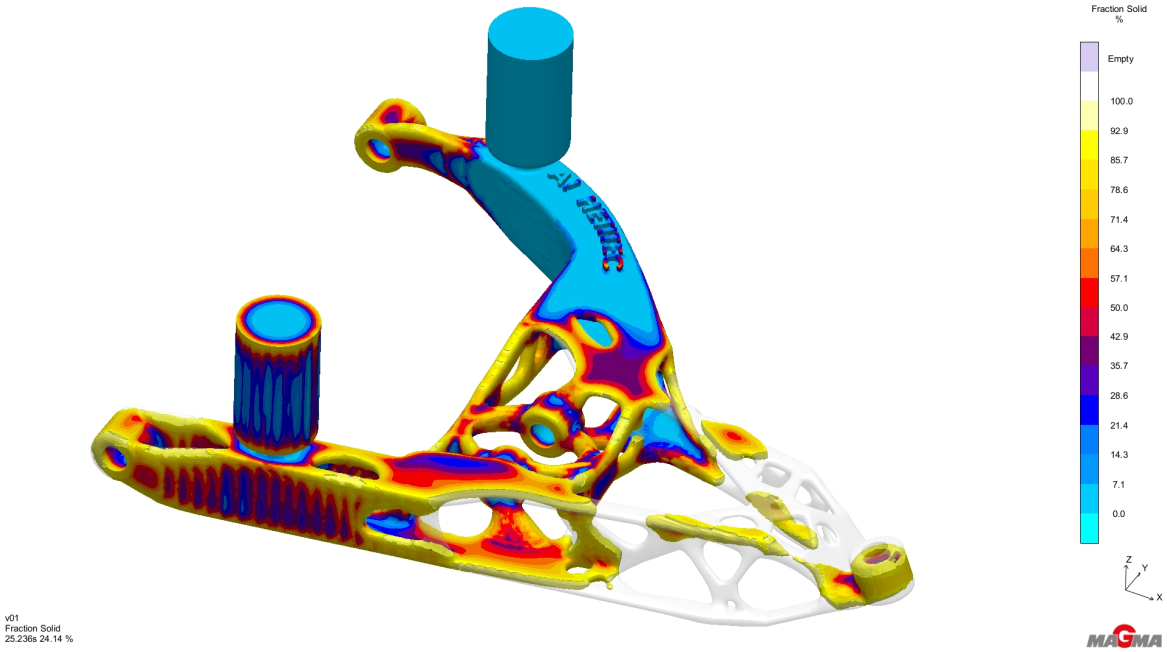
Fraction Solid
%
Empty
100.0
92.9
85.7
78.6
71.4
64.3
57.1
50.0
42.9
35.7
28.6
21.4
14.3
7.1
0.0
Z
Y
X
MAGMA
v01
Fraction Solid
25.236s 24.14 %

(b)

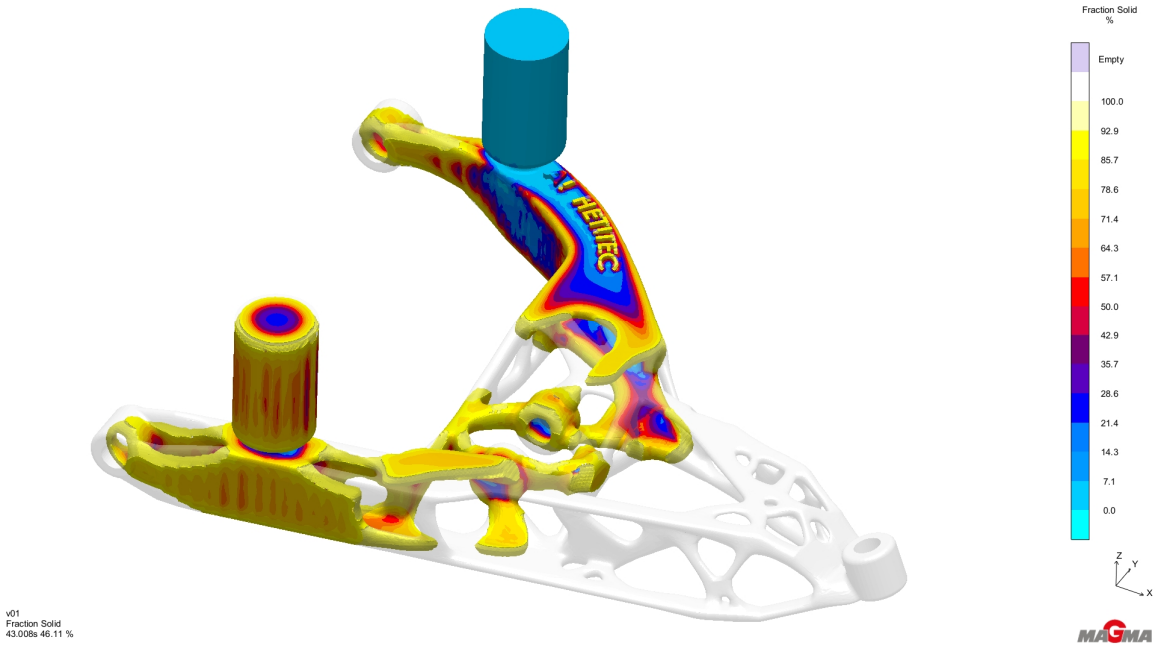

(c)

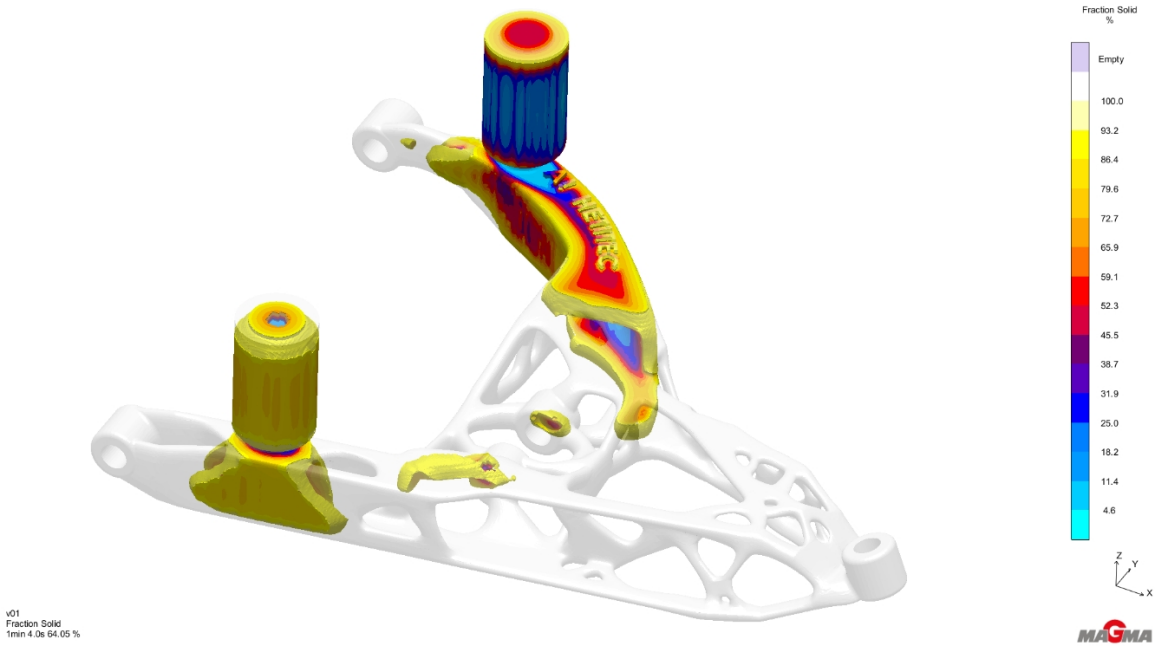

(d)

Figure 29: Time lapse of solidification in the lower A-arm mold

Although there are many porosity locations shown below in Figure 30 the porosity level is less than 10% for the vast majority of the areas. This probably will not cause a failed casting but this amount of porosity would likely not be acceptable in a finished product.

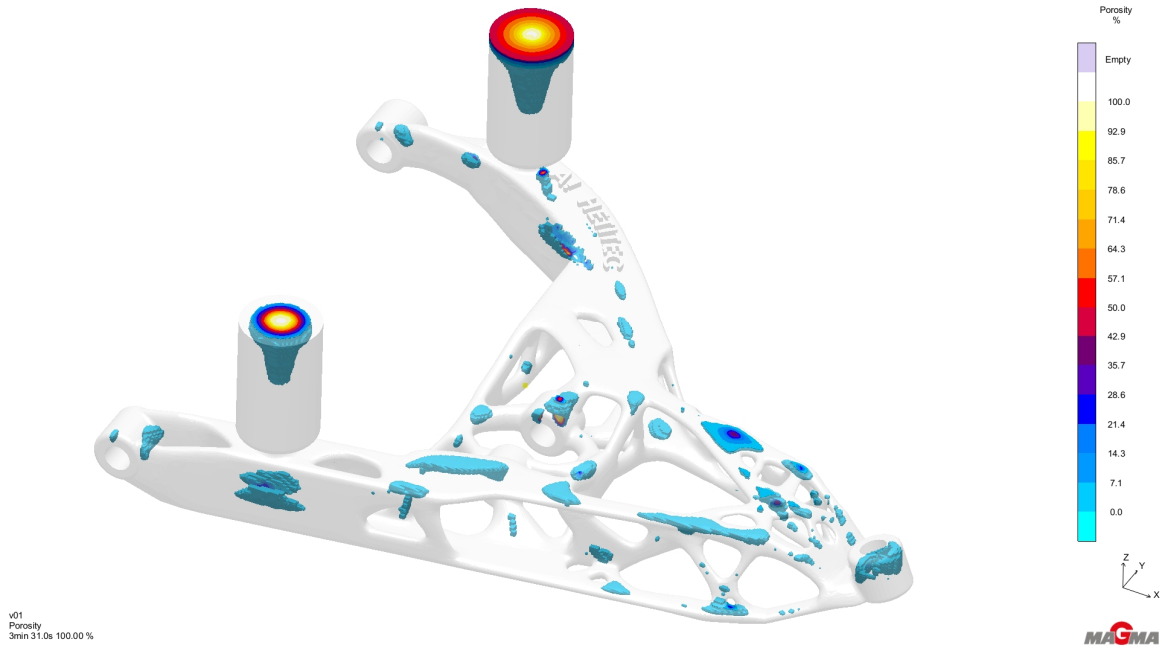

Figure 30: Simulated porosities in the lower A-arm

5 Casting Processes

5.1 Investment Casting

The design selected for investment casting was the propeller hub. This task was carried out entirely at Aalto University using its casting labs and machine shop. The procedure for casting is listed below:

1. 3D printed wax pattern and assembled
2. Attached appropriate casting features
3. Used assembly to fabricate mold
4. Burned out pattern
5. Poured into mold
6. Removed mold
7. Processed component

5.1.1 Pattern

The propeller hub was 3D printed using the new wax printer (3D Systems ProJet MJP 3600W) at the Aalto University campus. The component was printed at 1 to 1 scale, which was approximately 86.3 mm tall, by 120 mm wide. The original Propeller Hub design was altered slightly (Figure 31) in order to optimize the printing of the pattern[6] and to facilitate mold fabrication.

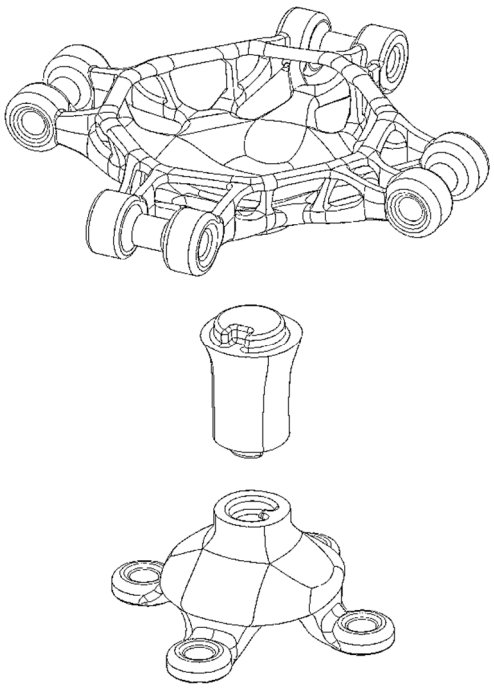

Figure 31: Propeller hub sections

[6] This was done mainly to reduce cost by minimizing the use of the relatively expensive wax and support material (approximately 600€ and 200€ per kilogram respectively). [39] [40]

The design was split into three sections in order to reduce the amount of support material that would be needed to print it as one piece. The holes in the feet were filled and the upper mounting holes were filled with a solid cylinder in order to facilitate proper flow during the pour.

The alternate design was printed at the lowest (of three) resolution setting of the wax printer. This was done mainly to save time. The printer is very accurate and produces a great surface finish, even at the lowest resolution setting. The print took 4 hours and 52 minutes and consisted of 1002 layers. The 'High Definition (HD) Mode' (lowest resolution setting) printed layers with a 32 µm thickness. The wax used was VisiJet M3 Hi-Cast and the support material used was VisiJet S400, both supplied by 3D Systems. [39]

The printed pieces were removed from the work-space platform (Figure 32) by placing them in a cooler at 7°C approximately. The different thermal expansion properties between the support material (white in color) and the aluminum plate caused them to separate after about 20 minutes of cooling. The support material was then removed by soaking the pieces in a 40°C bath of isopropyl alcohol.

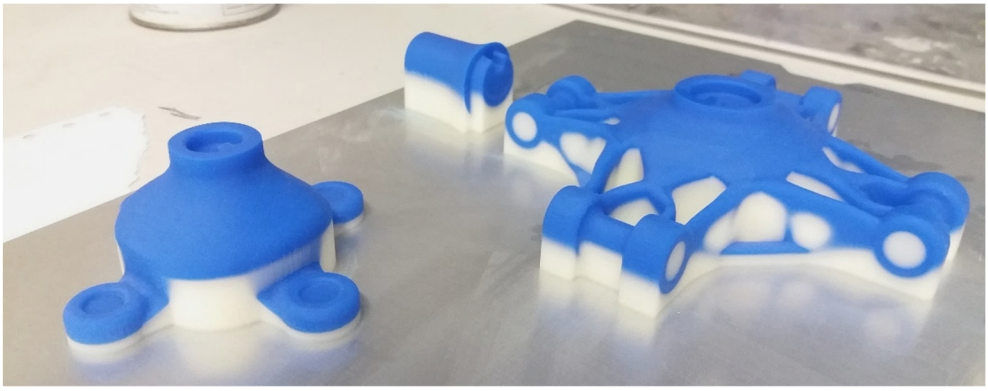

Figure 32: Propeller hub prints on the printer work-space platform

The three pieces were assembled and adhered by melting the bottom surface of the female end with a flat-bladed soldering iron, forming a small pool of liquid wax, then quickly joined together. A soft wax (workable with your hands at room temperature) was used to fill and smooth the seams.

5.1.2 Mold

Wax casting-component patterns (sprue, risers, runner, supports, etc.) were then attached to the assembled propeller hub print (Figure 33). This was done by melting the adjacent surface of the wax casting-component patterns with a flat-bladed soldering iron and quickly applying it to the desired surface of the 3D printed wax propeller hub.

Figure 33: Investment casting pattern assembly

This pattern assembly was then ready for mold fabrication. This was done by applying a layer of slurry to all outer surfaces. The appropriate sand was then applied evenly to the wet slurry. This was then hung up in an area with recirculating air to cure. Each layer was given a minimum of two hours for curing. Five layers of slurry and sand were applied (Table 3).

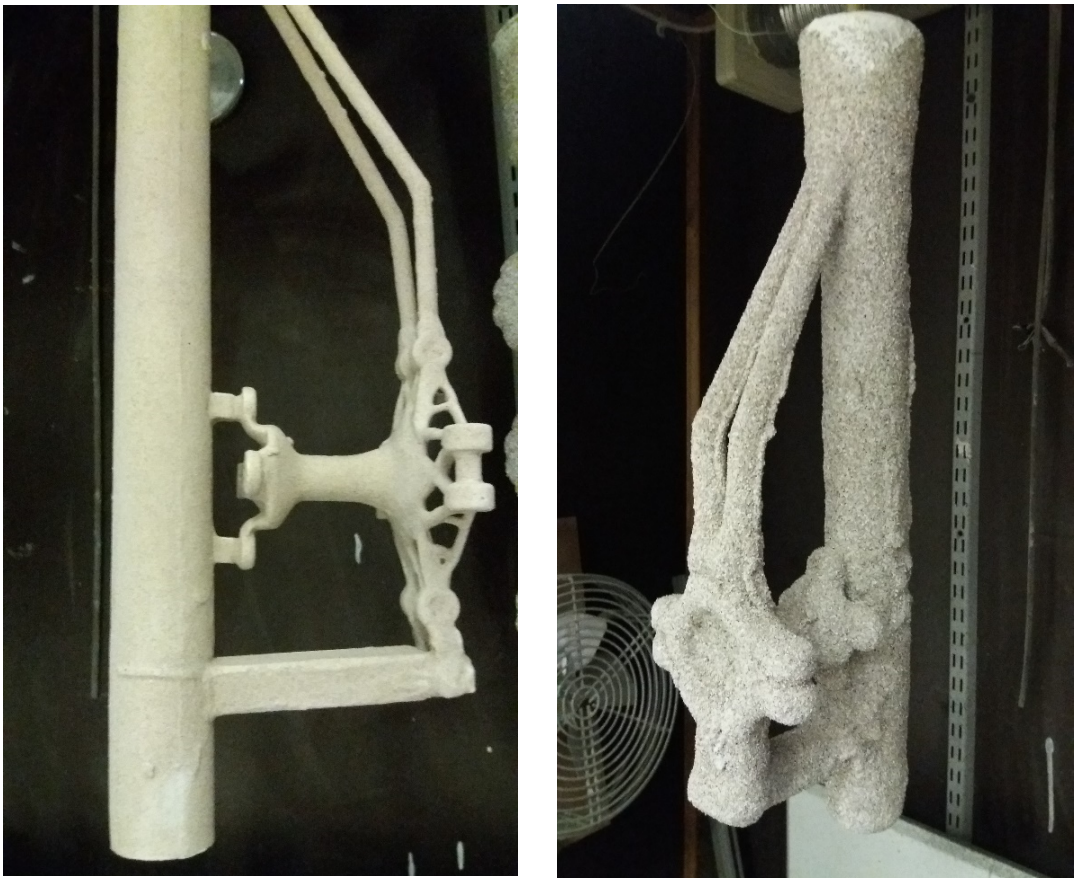

Figure 34: Pattern after first layer and after five layers respectively

Table 3: IC Mold Layer Specifications

Layer 1	Slurry and very fine zircon sand
Layer 2	Slurry and fine sand
Layer 3–5	Slurry and stucco

The cured mold was then ready for pattern burnout. This was accomplished by placing the mold upside-down in an electric furnace at 650°C for about 30 minutes (until all the wax had melted out). A metal tub below the furnace grate caught and collected the liquid wax for safe cooling. The furnace was then turned up to 750°C to further cure (firing) the empty ceramic mold. After 30 minutes (minimum) the mold was removed and placed in a container of sand. This sand acted as insulation in order to avoid premature cooling during the pour.

Figure 35: Mold in furnace for burnout and fired mold in sand respectively

5.1.3 Pour

The aluminum ingots (AlSi10) were placed in the induction furnace for melting during the same time that the wax burnout began. The molten aluminum was heated up to 750°C. Prior to pouring, the oxide layer that had separated to the top of the molten pool was removed and discarded. The crucible was then removed from the furnace to commence pouring.

Figure 36: During pour and after pour respectively

5.1.4 Processing

After proper cooling (about two hours) mold removal began. Most of the mold was removed initially by striking it with a mallet. In order to avoid damage to the propeller hub, the runner was the only area that came into contact with the mallet. Impact damage to the runner can be seen well in Figure 37. Vibration from striking the mallet to the runner caused the ceramic shell to break away from other adjacent sections. The more stubborn areas of ceramic shell were removed using a pressurized water jet.

Figure 37: Ceramic mold removal with mallet

The propeller hub was then separated from the runner and risers using a hacksaw. A metal file was used to remove and shape any excess material. The upper holes were also drilled out. The entire propeller hub was then sand blasted to give it a nice surface finish.

There were a few minor defects in the first pour. Porosity or bubbling was shown by the presence of three voids about 1 mm in diameter in various locations (two of them can be seen as small black spots in Figure 38). These defects were purely aesthetic. During removal (while using the hacksaw), one of the feet cracked and broke off. This was later reattached using a metal epoxy. Holes were not drilled in the four feet in order to avoid further damage.

Figure 38: Propeller hub after complete processing

5.1.5 Additional Castings

The decision to complete multiple castings of each of the two selected designs was made early in the progression of this work. This would help rule out anomalies in casting results, give opportunity for process improvement between iterations, and allow room for error if any would occur.

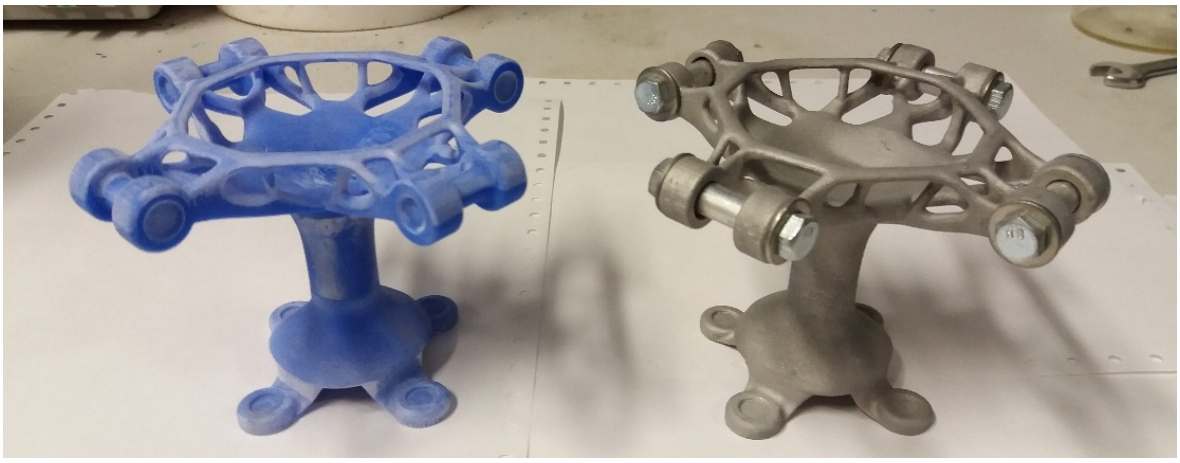

Figure 39: 3D printed wax propeller hub and cast aluminum propeller hub

The second propeller hub pattern was 3D printed and assembled in the same manner as the first. The wax casting-component patterns were also utilized in a similar manner. However, two additional risers were attached (Figure 40) with the intent to mitigate the porosity defects that formed on the first component. Some additional soft wax was also applied around the end points of the risers and filling channels to assist with filling and to minimize turbulence.

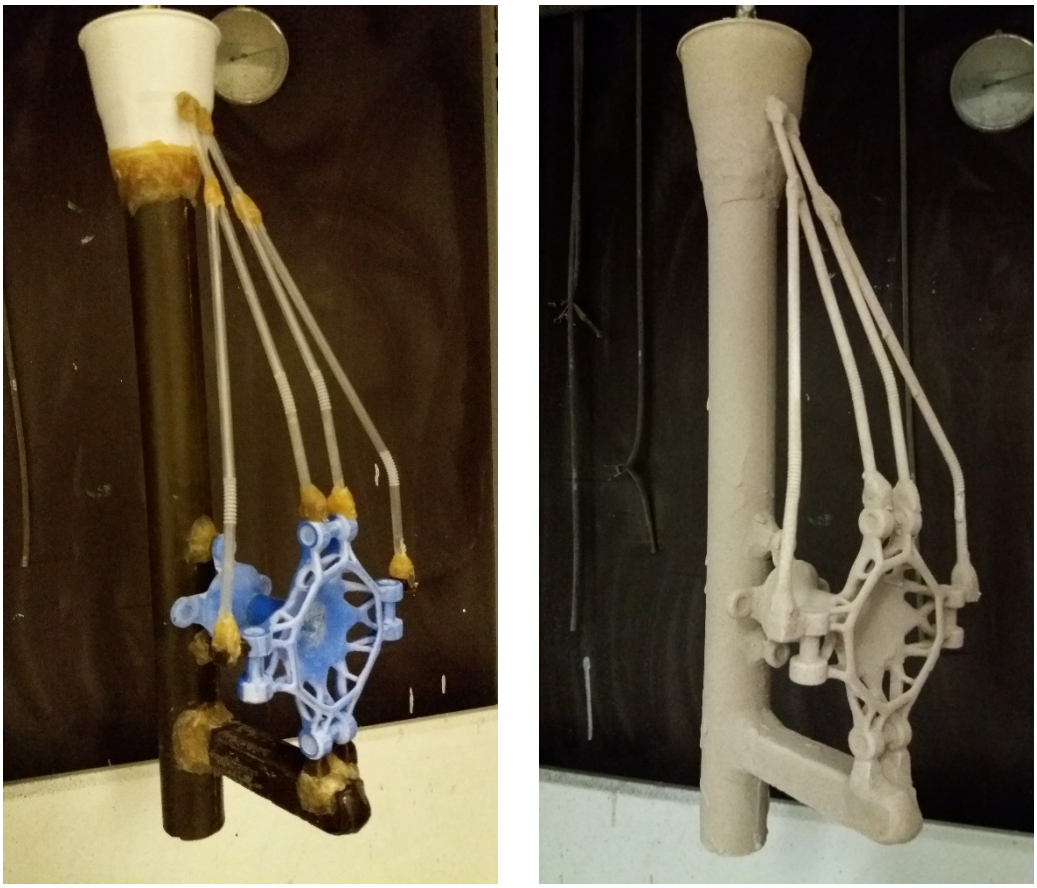

Figure 40: Propeller hub before and after first slurry/sand layer

Slurry and sand layers were applied similarly to the first casting (Table 3), consisting of five total layers with adequate curing of each one. The burnout, firing, and pouring processes were also carried out in a similar manner. Removal of the component from the runner and risers was accomplished using a pneumatic oscillating saw. This proved to be a less stressful cutting process than when using the hacksaw. It was anticipated that the use of this saw would avoid breaking any part of the component. However, cracks were already present in two of the legs (Figure 41) and observed immediately after the ceramic mold was removed[7]. One of the legs separated at the crack site during removal. This was later reattached using a metal epoxy.

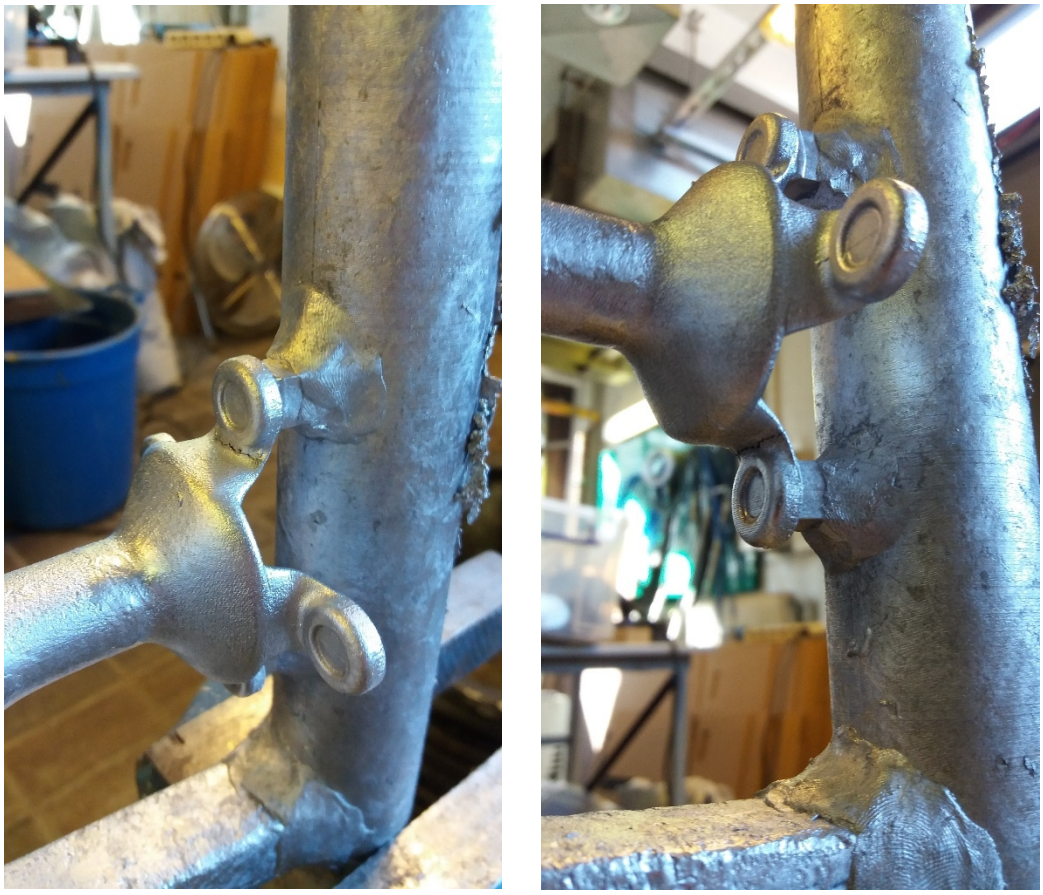

Figure 41: Visible cracks on two legs of the second propeller hub IC

5.2 3D Printed Sand Mold Casting

The design selected for 3D printed sand mold casting was the lower A-arm. The molds will be fabricated[8] (according to the supplied design) by the Finnish company Hetitec and transported to Aalto University for casting and processing.

[7] Possible causes are discussed in the Results section.

[8] Timeline constraints did not allow the casting of the lower A-arm to be reported in this work (procedure steps 2 – 7). Although not reported in this work, the lower A-arm will still be fabricated.

The procedure for casting is listed below:

1. Designed mold (two iterations)
2. 3D printed sand molds at Hetitec
3. Transported molds to Aalto University
4. Assembled mold
5. Poured into mold
6. Removed mold
7. Processed component

Unlike the molds used in the IC process, the fabrication of 3D printed sand molds does not require any patterns or other consumable features.

5.2.1 Mold: Version 1

The next step after finalizing the lower A-arm model was to design the mold. Parting lines, sprue location and geometry, riser location and geometry, and overall mold dimensions were the key features that needed to be defined.

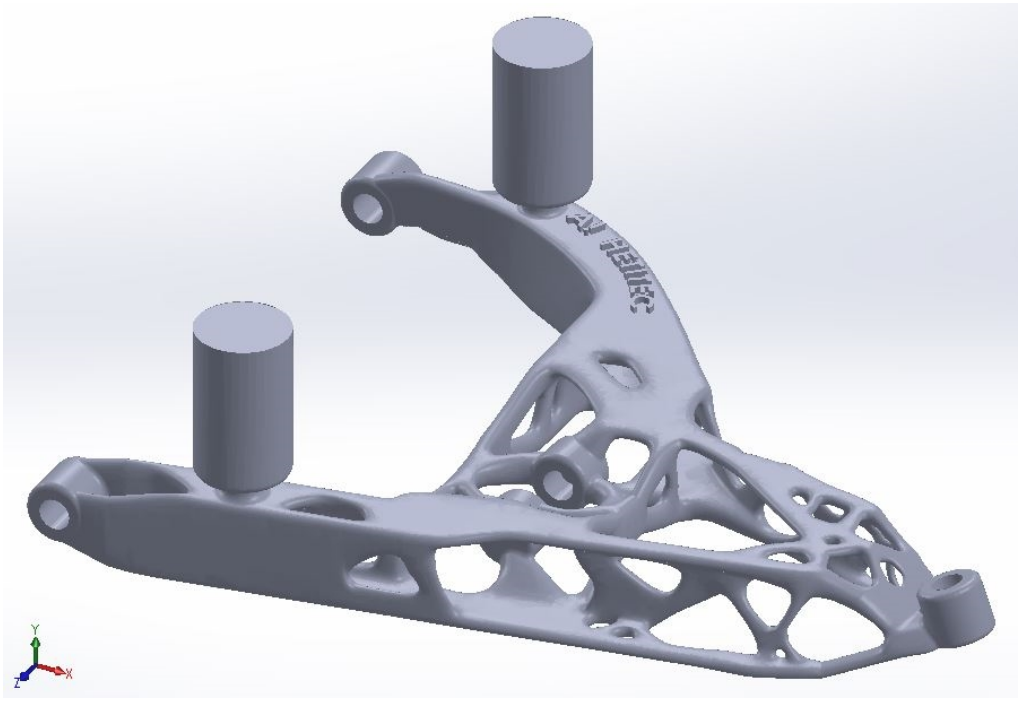

Figure 42: Lower A-arm with sprue, riser, and logos

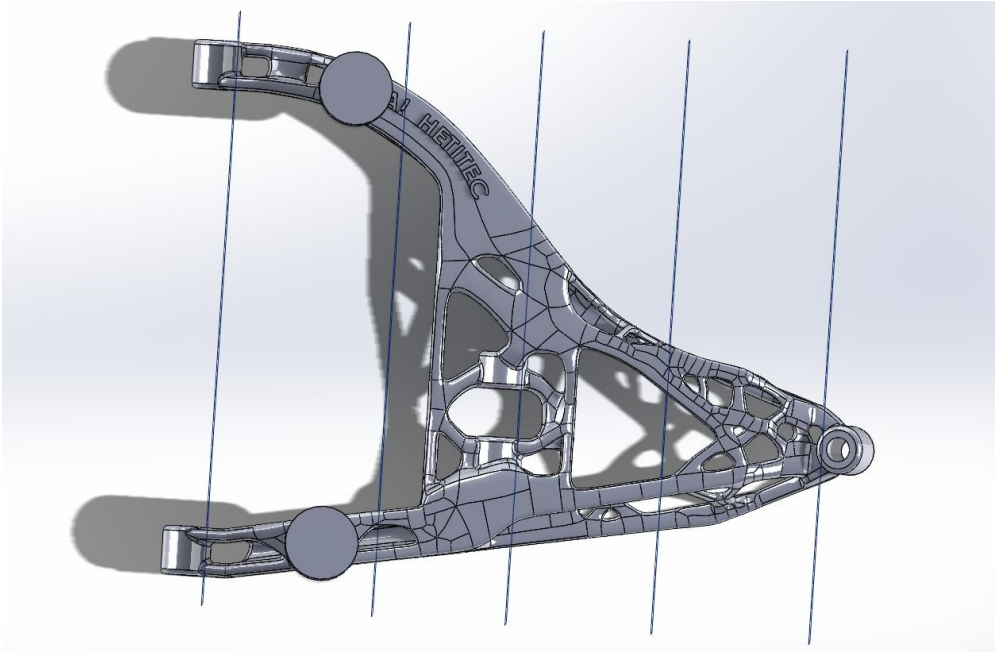

Figure 43: Mold parting lines

Due to the complexity of the lower A-arm's geometry, the mold was split into six sections (five parting lines). These smaller mold sections would facilitate the removal of loose sand after printing. Larger sections would risk trapping loose sand in the printed mold, especially in small passages.

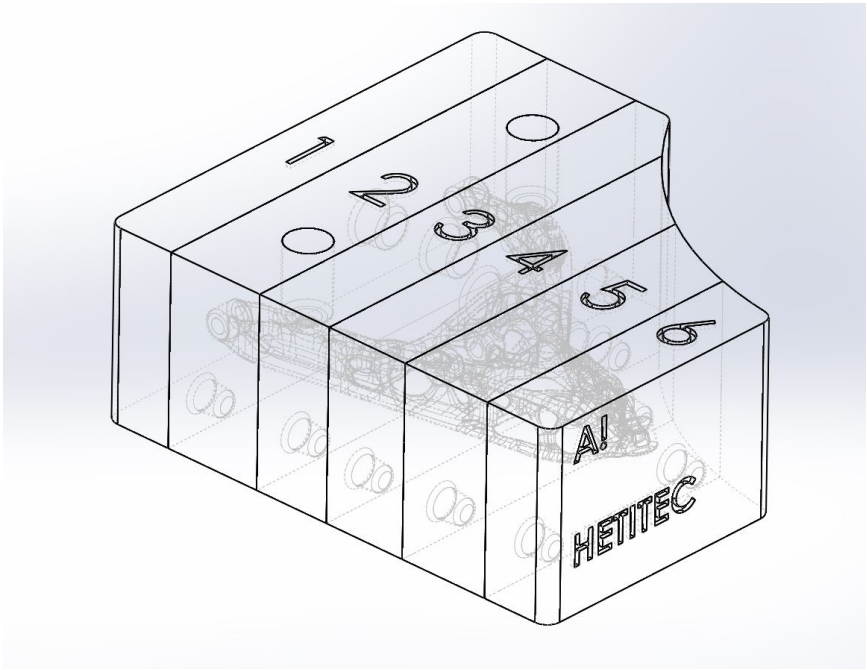

Figure 44: Transparent assembly of mold sections

A relief was added to the mold design (top-right section of the mold in Figure 44) in order to reduce cost and production time.

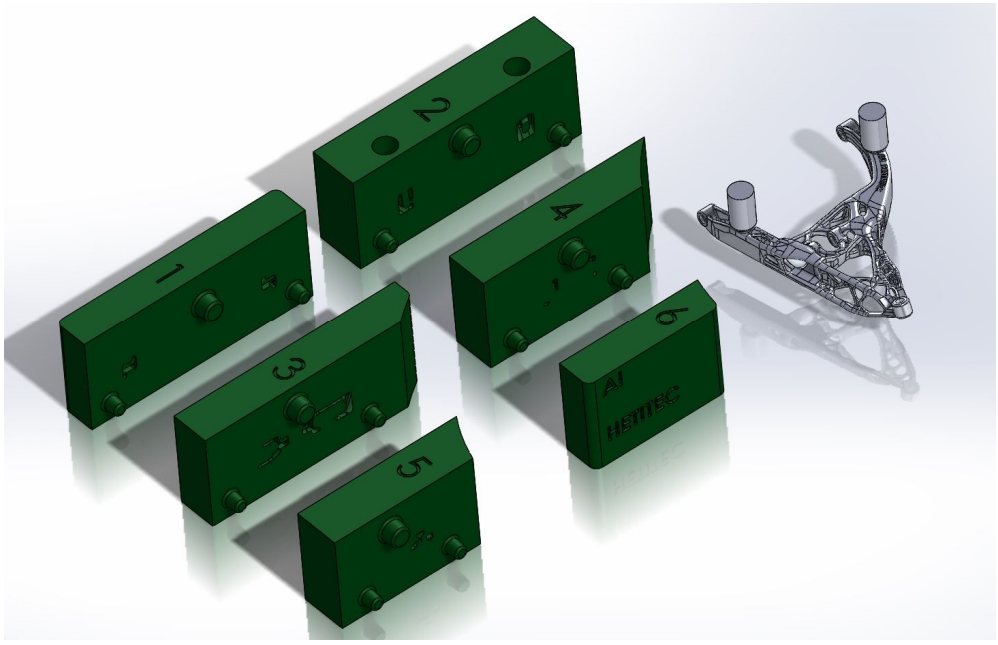

Figure 45: Exploded view of lower A-arm and mold sections

5.2.2 Mold: Version 2

After their analysis of the mold design, Hetitec voiced concern about excess sand removal. Splitting the mold into more sections (additional parting lines) would be the best way to remedy the problem. The second mold design, now with 17 sections, is shown in Figure 47 and Figure 48.

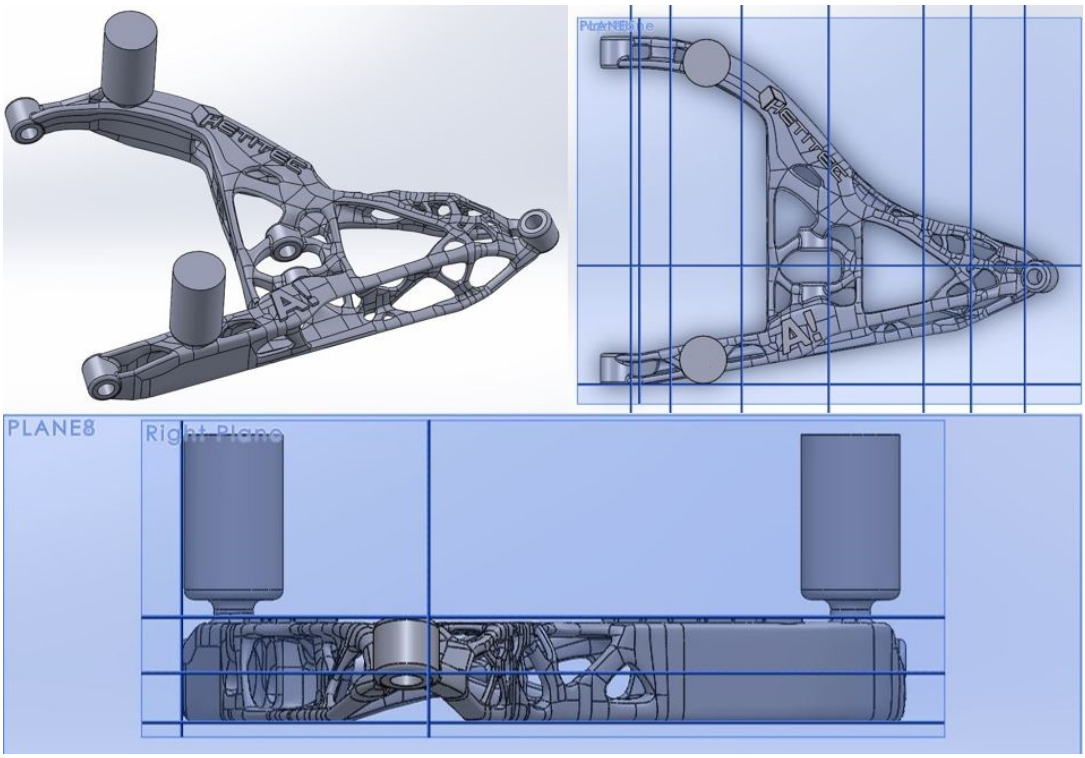

Figure 46: Lower A-arm and new parting lines

The additional parting lines cause the mold sections to be smaller in size which separates and decreases the length of small channel features. These smaller mold sections should facilitate the removal of excess sand after they are printed.

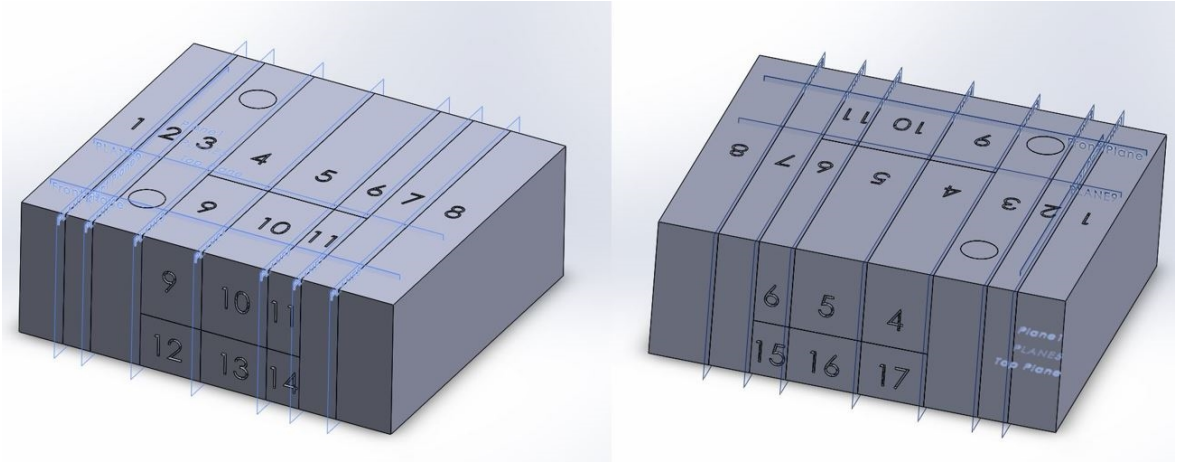

Figure 47: Lower A-arm mold version 2

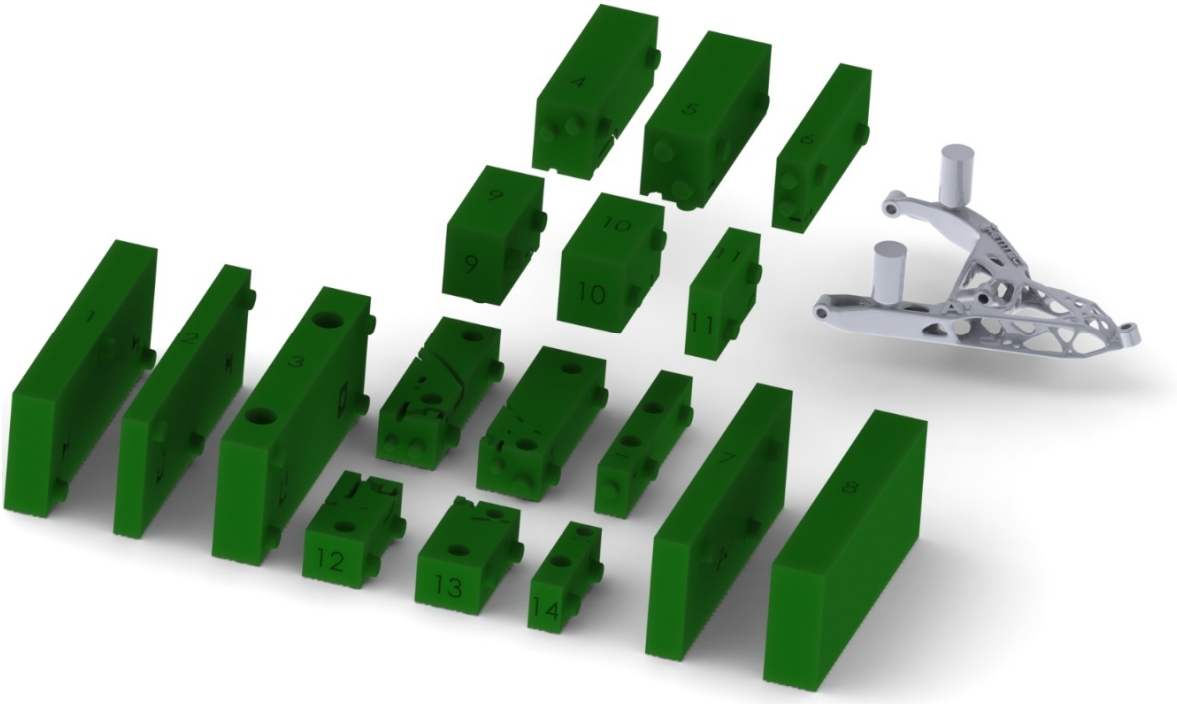

Figure 48: Exploded view of lower A-arm and mold version 2 sections

Figure 49: Lower A-arm with logos

Hetitec will fabricate the 3D printed sand molds for the lower A-arm at their facility in Tampere, Finland. They will be fabricated in accordance to the design provided by this work (Figure 48 and Figure 49).

6 Results

The results of the component designs, simulations, and investment castings of the propeller hub were mostly positive. Timeline constraints did not allow the casting of the lower A-arm to be reported in this work. However, the simulation results for the lower A-arm showed that casting the component should be successful.

6.1 Design

The component designs turned out well and were useful in many ways. The array of models ranged from simple geometry with simple loading to complex geometry with complex loading. This allowed for vast optimization variance and helped to improve understanding of Inspire's functionality.

The selected designs (propeller hub and lower A-arm) turned out very nicely and fit very well with their corresponding casting processes. The topology optimizations met the design requirements of high geometric complexity and good castability. These selected designs were then finished using polyNURBS and processed for casting.

6.2 Simulations

The simulations of the propeller hub and lower A-arm turned out well and were insightful. Both components were subjected to simulations of molten flow velocity, molten flow temperature, solidification characteristics, and porosity using Magma.

The simulations of the propeller hub yielded mostly positive results. They showed mild turbulence and even cooling without the presence of drastic hot or cold spots. Solidification of the propeller hub occurred initially in multiple isolated areas due to the great size differences between adjacent bodies, which can lead to internal stresses and cracking. The porosity results were positive, showing very few porosity locations with very low porosity level.

The simulations of the lower A-arm were decent but with a higher chance of complication due to its geometric complexity. The presence of multiple flow fronts and the smaller features near the 'point' of the lower A-arm cause some turbulence and large temperature variance throughout the component. Solidification also occurs initially in many isolated areas, which is not ideal. Many small porosity spots occur throughout the component but are of low porosity level. Though some of these simulations raise concern, casting of the lower A-arm should be possible.

6.3 Investment Casting

Two propeller hub castings were produced during this work, both from the same design. The only difference between the two castings was the additional risers on second mold.

The results of first IC of the propeller hub were quite good. All features of the component were complete and the surface finish was great overall, reflecting the surface of the wax print very accurately as seen in Figure 50. A few voids and protrusions were present. The voids were likely formed from air pockets in the molten aluminum while the protrusions may have developed from defects in the initial slurry/sand layers.

The results of the second IC of the propeller hub were also quite good. It did, however, contain more defects overall. There was more porosity-spots and about same amount of protrusions as the first casting. The most significant defects were the presence of two cracks, one on each of two opposing legs. More notably, these two legs were the fill sites for the lower section of the propeller hub. One of these legs separated at the crack site during removal from the runner (Figure 50). The other two free-hanging legs showed no signs of cracking on both the first and second propeller hub castings.

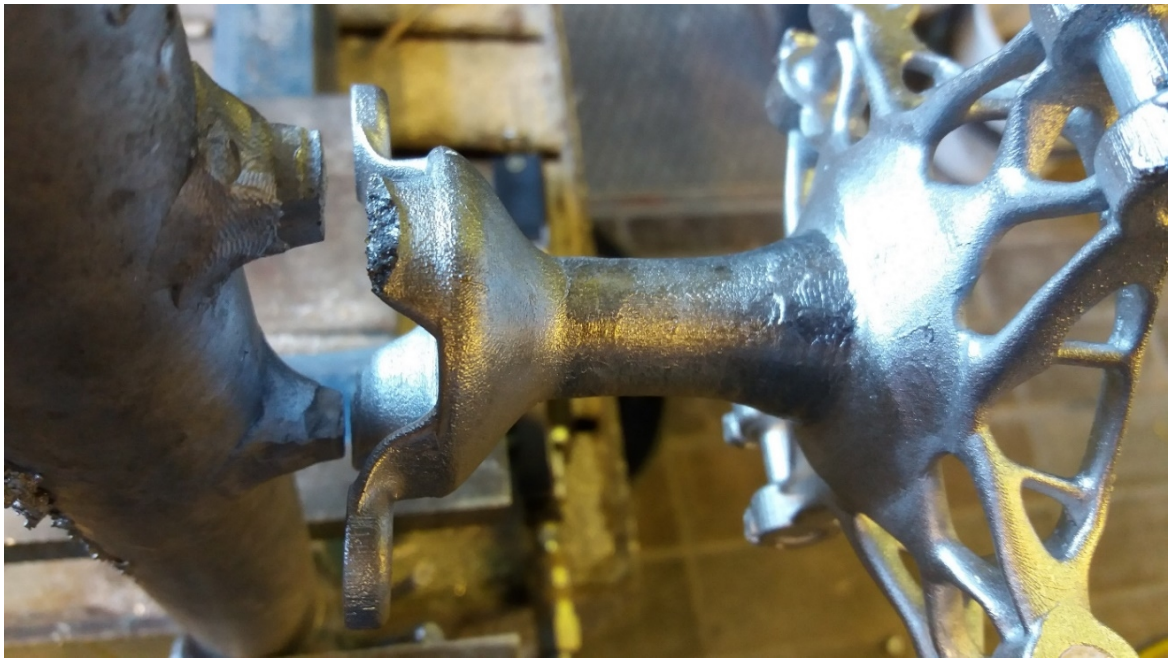

Figure 50: Broken leg during removal of second IC of propeller hub

Further contemplation concluded that local premature cooling likely caused the cracking. These legs are very thin features and cool much quicker than the two larger bodies (the runner and the base/body of the propeller hub) on either side of them. Once the leg section had solidified, persisting contraction on either side of the leg introduced tension stresses that caused crack formation. This theory brought to mind the first propeller hub IC. Although no cracking was observed on any of the legs of the first propeller hub IC prior to removing the runner, internal cracks may have been present. This would have facilitated the separation of the leg during runner removal with the hacksaw.

7 Discussion

The results of this work were very positive. Many different designs were created, reviewed, selected, and processed for casting. The investment casting of both of the propeller hubs was successful, therefore proving the ability to cast topologically optimized components. Although the capabilities of the 3D printed sand mold for the casting of the lower A-arm could not be reported in this work, the component design and mold design were both created and prepared for use. Casting simulations of both components were successful and insightful.

7.1 Topology Optimization

The optimization software used during this work was Inspire 2017 from solidThinking. The program contains various tools for feature creation, topology optimization, structural analysis, and post processing. A basic tutorial is offered online for new users.

7.1.1 Capabilities

Inspire is a versatile program that allows model optimizations to be tailored for many applications. Load types such as point, surface, and moment can be applied with varying directions and magnitudes. Many support options are also available. These loads and supports are saved as a 'load case' in the model tree. Many different load cases can be created for the same model. Loads and supports can be defined individually or they can be shared between load cases when there are redundant parameters. All of these abilities make comparison between different optimizations quick and easy.

The optimization function also has many parameters that can be adjusted as needed. The core objective is to optimize the model according to mass or stiffness. For this work, optimizing for max stiffness provided the most desirable results. The model's mass is still manipulated since performing the max stiffness method requires the target mass percentage to be defined. Minimum and maximum wall thickness can also be established. This is quite useful since wall thickness can be a critical feature when casting products. Defining minimum wall thickness is also a way of indirectly affecting the resolution of the optimization. Smaller wall thicknesses, for example, allow more voids, tendrils, and other features to develop during optimization. The side effect to this is longer run times. Defining the minimum wall thickness at 4 mm – 6 mm required a run time of approximately 20 minutes for most models.

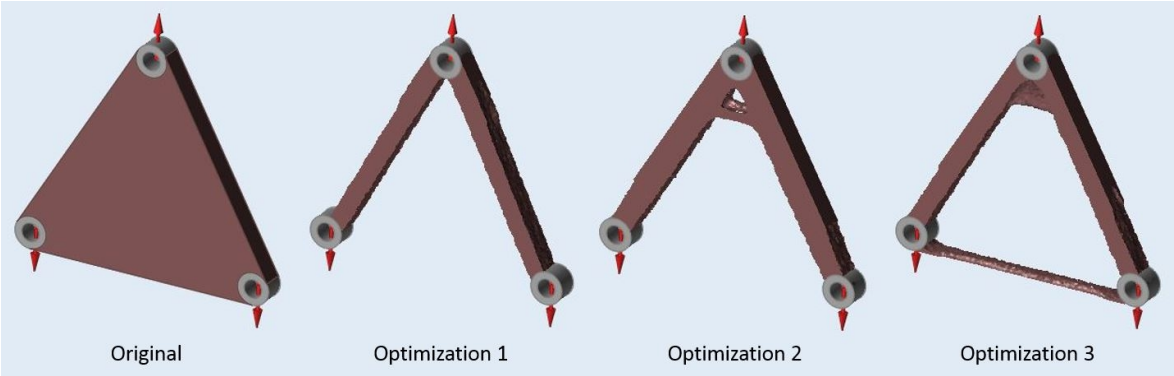

Figure 51: Triangular bracket with 2D tension forces

All of these parameters (loads, supports, target mass, wall thickness) can vary the optimization results dramatically. Figure 51 , for example, shows a few optimization results of a simple component with simple loading. The only differences between the three optimizations were the load magnitudes and target mass percentage.

7.1.2 Limitations

Inspire has some limitations and was occasionally difficult to work with. The need for load balancing made some desired load cases impossible or time-consuming to apply. This inconvenience was avoided by defining at least one support parameter. The support parameter kept the model mounted and stationary in the presence of unbalanced forces. Applying multiple supports, however, was often a disadvantage because this sometimes caused the bodies between support locations to be isolated from the applied forces. This often resulted in the absence of geometry between supports.

7.2 Post-Optimization

The polyNURBS tool in Inspire provides the ability to smooth the rough polygonal surfaces (Figure 52) that result from the topology optimization. The tool works similar to lofting tools found in 3D CAD programs by using selected cross-sections of the optimized geometry as the sketch shapes for the loft. These smoother surfaces are beneficial for both the design aesthetic goals and the component castability.

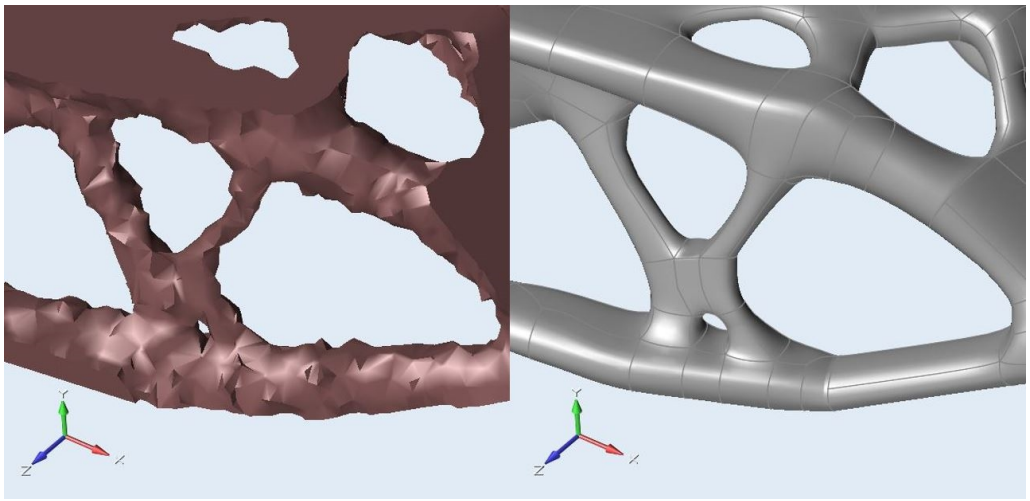

Figure 52: Surface finish: optimized-only and optimized with polyNURBS

7.2.1 Capabilities

The polyNURBS tool is relatively easy to use while also providing deep levels of customization if desired. Lofted sections are created by clicking a cross section, dragging the cursor along the feature, and clicking again to select the end cross section. The dimensions and shape of these bodies can be adjusted arbitrarily by clicking and dragging the curser or more precisely by entering a numerical value measured in meters[9]. Body surfaces can be flattened, aligned (to other faces or normal to X,Y, or Z plane), translated, and rotated.

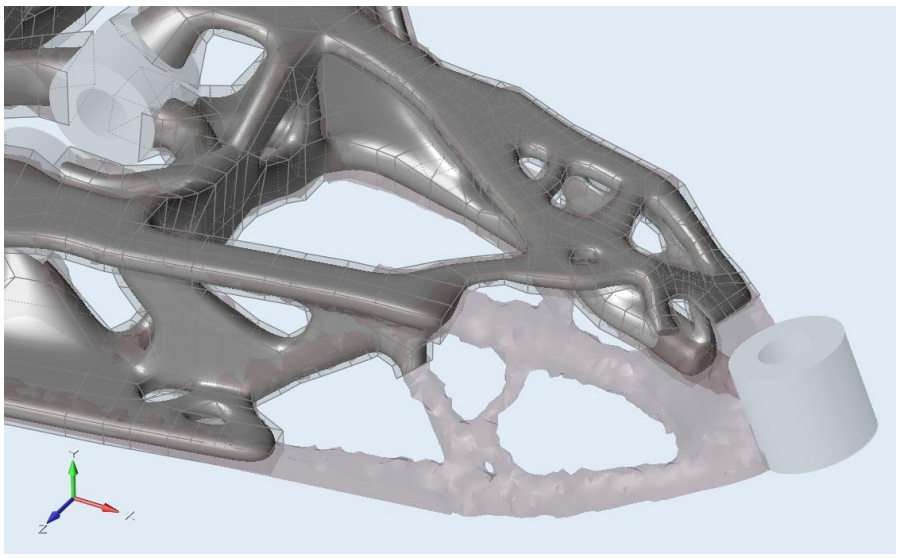

Figure 53: Partially completed polyNURBS on the lower A-arm

[9] The minimum unit of length was actually sub-millimeter. The finest unit observed was 0.0001 m (0.1 mm).

7.2.2 Limitations

The polyNURBS tool was sometimes difficult to use and caused a few problems during this work. The main issue appeared during post-optimization processing when the steering knuckle, propeller hub, and lower A-arm were imported into Creo Parametric from Inspire for casting preparation. Creo Parametric was constantly reporting model build errors, making it very difficult to work with. The errors were caused by intersecting geometries between the optimized features and the partitions. These intersections were caused by the functionality of polyNURBS; the tool does not allow lofting directly to an outer partition surface. The loft geometry created has to be manually placed inside the target partition body (seen by the hidden lines in the two cylindrical partitions in Figure 54). This problem was alleviated by using the Boolean tool in Inspire to combine features in order to remove the intersecting geometry.

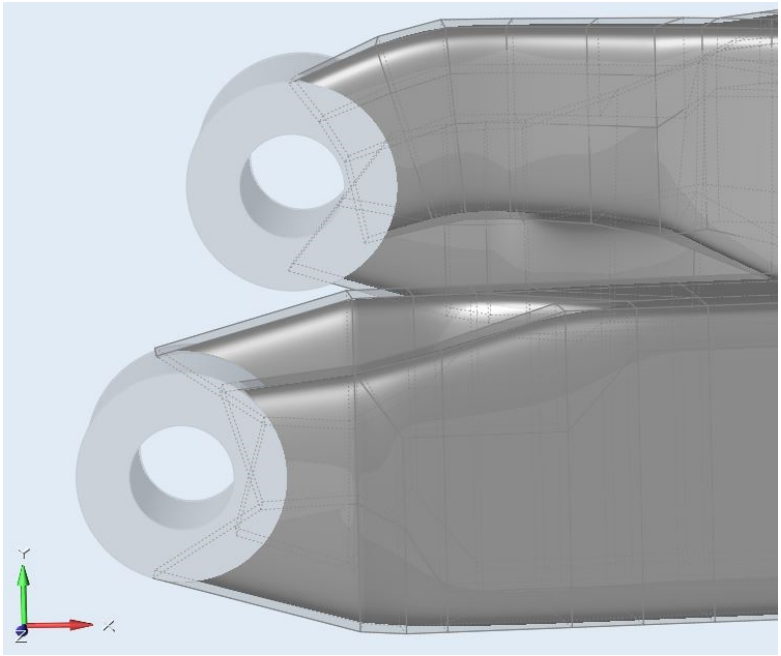

Figure 54: Intersecting geometry between partitions and polyNURBS

Inspire was sometimes very buggy when using polyNURBS. For example, individual polyNURBS loft body sections would fail to respond properly to commands at random times. The most frequent example of this was when using the +/- tool. The function of this tool is to add a generic loft body to an existing loft surface (without having to select the second cross section) or to remove a previously created loft body. The problem was that loft bodies sometimes failed to delete correctly. Instead of removing the selected loft body, the section would become hollow (often protruding through other adjacent loft bodies) with the outside surface remaining. The only way to delete the corrupted loft body was to first delete all of the attached geometry. Inspire was also prone to random and complete program crashing when using polyNURBS. These bugs seemed to appear more frequently with increasingly complex geometry. Though the online tutorial was helpful for getting started, it was too basic for experienced users. Unlabeled tools and the lack of a keyboard shortcut glossary hid many useful functions.

7.3 Investment Casting

The investment castings (two of them) were completed successfully and with only a few minor complications. One issue was the difficulty of mold application and removal due to the complex geometry of the propeller hub. The many small features (and small gaps between them) made application of the slurry and sand layers very tedious. These layers demanded very disciplined application in order to achieve even and complete coating and to avoid defects such as air pockets. These complex and small features also made mold removal (after the pour and proper cooling) very difficult. Removal of much of the mold required the use of a high-pressure water jet.

7.4 Casting Feasibility

The collaboration of casting and AM technologies to directly manufacture topologically optimized components has proven to be a feasible practice. Three-dimensional printing methods such as FDM and 3D sand mold printing facilitate the casting of the complex geometries that often result from topology optimization. This work has shown that such components can be produced successfully with minimal design alteration and little deviation from typical casting processes.

However, the geometric complexity of topologically optimized components increases the chances of complications such as porosity, voids, cracking, and difficult mold removal. Multiple flow fronts and large variances in adjacent body sizes are the main cause of some of these complications. Many of these problems may be avoided with future improvements to design and to casting processes.

7.5 Future Considerations

One area that has much room for improvement (and iterative testing) is the casting design and process. Since this work was focused on testing the possibility of casting topologically optimized components with little or no alteration to the component optimization, little focus was given to optimizing the casting process. The next step of study in this area would be the optimization of the casting process when fabricating topologically optimized components. This optimization could focus on the casting simulations, the mold design, or both. Optimizing the mold design could address things such as sprue and riser details (number of features and their locations), 3D printed sand mold parting line details (number of parting lines and their locations), mold treatments, and many other parameters. This type of testing could be used iteratively with the simulations in order to optimize the casting process of such complex components.

References

[1] G. Rozvany, "Aims, scope, methods, history, and unified terminology of computer-aided topology optimization in structural mechanics," *Struct Multidisc Optim,* 2001.

[2] M. Molitch-Hou, "Frustum Topology Optimization Integrated into Siemens NX for 3D Printing," http://www.engineering.com/3DPrinting/3DPrintingArticles/ArticleID/14633/Frustum-Topology-Optimization-Integrated-into-Siemens-NX-for-3D-Printing.aspx?e_src=relart [10.4.2017].

[3] GrabCAD, "The Generate Quadcopter Challenge," https://grabcad.com/challenges/the-generate-quadcopter-challenge [10.4.2017].

[4] L. B. Hunt, "The Long History of Lost Wax Casting," Johnson Matthey & Co. Limited.

[5] "Investment Casting Wax," *Westech Wax Products,* http://www.westechwax.com/investment-casting-wax/ [10.4.2017].

[6] J. Campbell, Complete Castings Handbook, Elsevier Ltd., 2011.

[7] M.-K. Hassiotis, "Investment Casting vs. Die Casting: 7 Considerations When Choosing a Process," http://news.ewmfg.com/blog/investment-casting-vs.-die-casting-considerations-when-choosing-process [10.4.2017].

[8] "Sand Casting," *Mechanica Technical Solutions,* http://www.mechanicatech.com/Casting/sandcasting.html.

[9] S. Boonmee, B. Gyesi and D. M. Stefanescu, "Casting Skin of Compacted Graphite Iron Part I: Evaluation and mechanism of formation," *American Foundry Society,* 2010.

[10] "Hüttenes-Albertus - The Foundry in the Age of Industry 4.0: New plant technology requires new materials," http://www.foundry-planet.com/equipment/detail-view/huettenes-albertus-the-foundry-in-the-age-of-industry-40-new-plant-technology-requires-new-materials/?cHash=7e6b65122d508ab9ed95c15aa5060733 [10.4.2017].

[11] S. O. Onuh and Y. Y. Yusuf, "Rapid prototyping technology: applications and benefits for rapid product development," *Journal of Intelligent Manufacturing,* 1999.

[12] N. Guo and M. C. Leu, "Additive manufacturing: technology, applications, and research needs," *Front. Mech. Eng.,* pp. 215-243, 2013.

[13] M. L. Griffith and J. W. Halloran, "Freeform Fabrication of Ceramics via Stereolithography," *J. Am. Ceram. Soc.,* 1996.

[14] C. Zhou and Y. Chen, "Calibrating Large-area Mask Projection Stereolithography for Its Accuracy and Resolution Improvements," 2009.

[15] H. Li, J. Chen, K. Chandrashekhara, M. Xu, S. N. Lekakh and V. L. Richards, "Characterization and modeling of anisotropic SL pattern during investment casting process," *Int J Adv Manuf Technol,* 2015.

[16] X. Gu, J. Zhu and W. Zhang, "The lattice structure configuration design for stereolithography investment casting pattern using topology optimization," *Rapid Prototype Journal,* 2012.

[17] C. Groth, N. D. Kravitz, P. E. Jones, J. W. Graham and W. R. Redmond, "Three-Dimentional Printing Technology," 2014.

[18] L. Froyen and M. Rombouts, "Binding mechanisms in selective laser sintering and selective laser melting," *Rapid Prototyping Journal,* 2005.

[19] P. Jain and A. M. Kuthe, "Feasability Study of manufacturing using rapid prototyping: FDM Approach," *Procedia Engineering,* 2013.

[20] R. Singh and S. Singh, "Experimental investigations for statistically controlled solution of FDM assisted Nylon6-Al-Al2O3replica based investment casting," *Materials Today: Proceedings,* 2015.

[21] C. M. Cheah, C. K. Chua, C. W. Lee, C. Feng and K. Totong, "Rapid prototyping and tooling techniques: a review of applications for rapid investment casting," *International Journal of Advanced Manufacturing Technology,* pp. 308-320, 2004.

[22] C. W. Lee, C. K. Chua, C. M. Cheah, L. H. Tan and C. Feng, "Rapid investment casting: direct and indirect approaches via fused deposition modelling," *Int J Adv Manuf Technol,* pp. 93-101, 2004.

[23] R. Singh, S. Singh and G. Singh, "Dimensional Accuracy Comparison of Investment Castings Prepared With Wax and ABS Patterns for Bio-Medical Application," *Procedia Materials Science ,* 2014.

[24] M. Macků and M. Horáček, "Applying RP-FDM Technology to Produce Prototype Castings Using the Investment Casting Method," *Archives of Foundry Engineering,* 2012.

[25] C. Liu, S. Jin, X. Lai, B. He and F. Li, "Influence of complex structure on the shrinkage of part in investment casting process," *Int J Adv Manuf Technol,* 2015.

[26] "The Main Properties of PLA and ABS Compared," https://all3dp.com/pla-abs-3d-printer-filaments-compared/ [10.4.2017].

[27] W. Wanlong, J. G. Conley and H. W. Stoll, "Rapid tooling for sand casting using laminated object manufacturing process," *Rapid Prototyping Journal,* vol. 5, pp. 134-141, 1999.

[28] E. S. Almaghariz, B. P. Conner, L. Lenner, R. Gullapalli, G. P. Manogharan, B. Lamoncha and M. Fang, "Quantifying the role of part design complexity in using 3D sand printing for mold and cores," 2016.

[29] R. Singh, "Three Dimensional Printing for Casting Applications: A State of Art Review and Future Perspectives," *Advanced Materials Research,* 2010.

[30] B. Berman, "3-D printing: The new industrial revolution," *Business Horizons,* pp. 155-162, 2012.

[31] T. Rayna and L. Striukova, "From rapid prototyping to home fabrication: How 3D printing is changing business model innovation," *Technological Forecasting & Social Change,* pp. 214-224, 2015.

[32] M. Chhabra and R. Singh, "Rapid casting solutions: a review," *Rapid Prototyping Journal,* vol. 17, no. 5, pp. 328-350, 2011.

[33] D. Snelling, H. Blount, C. Forman, K. Ramsburg, A. Wentzel, C. Williams and A. Druschitz, "The effect of 3D printed molds on metal castings".

[34] "Hetitec 3D-Printing," http://hetitec.com/ [24.4.2017].

[35] D. Snelling, Q. Li, N. Meisel, C. B. Williams, R. C. Batra and A. P. Druschitz, "Lightweight Metal Cellular Structures Fabricated via 3D Printing of Sand Cast Molds," *Advanced Engineering Materials,* no. 7, 2015.

[36] "What Foundries Have to Know About 3D-Printing," http://www.voxeljet.com/unternehmen/news/das-muessen-giessereien-ueber-den-3d-druck-wissen/ [10.4.2017].

[37] L. Krog, A. Tucker and G. Rollema, "Application of Topology, Sizing and Shape of Optimization Methods to Optimal Design of Aircraft Components," Altair Engineering, Bristol, 2002.

[38] C.-Y. Lin, T. Wirtz, F. LaMarca and S. J. Hollister, "Structural and mechanical evaluations of a topology optimized titanium interbody fusion cage fabricated by selective laser melting process," WILEY InterScience, 2007.

[39] "ProJet MJP 3600W & 3600W Max," 3D Systems, Inc., 2016.

[40] advantage, "VisiJet M3 Hi-Cast RealWax," https://www.advantagelitho.com/3d-visijet-m3-hicast-realwax-material.html [5.4.2017].

[41] advantage, "VisiJet S400 Support Material," https://www.advantagelitho.com/3d-visijet-s400-support-material.html [5.4.2017].

[42] C. Gosselin, R. Duballet, P. Roux, N. Guadillière, J. Dirrenberger and P. Morel, "Large-scale 3D printing of ultra-high performance concrete – a new processing route for architects and builders," *Materials and Design,* pp. 102-109, 2016.